https://doi.org/10.5194/egusphere-2026-6100
Preprint. Discussion started: 11 November 2026
© Author(s) 2026. CC BY 4.0 License.

Landsat archives, a key source for disentangling the complex anthropogenic controls of large river changes

Shalini Singh[1], Rey Louis[2], Nikita Karnatak[1], Barbara Belletti[3], Herve Piegay[2], Vikrant Jain[1]

[1]Department of Earth Sciences, Indian Institute of Technology, Gandhinagar, 382355, India
[2] ENS de Lyon, Lyon, 60342, France
[3]CNRS-The French National Centre for Scientific Research, Paris,75794, France

Correspondence to: Vikrant Jain(vjain@iitgn.ac.in)

Abstract

River form reflects the balance of water and sediment fluxes acting on an inherited geological and climatic template; where human activity alters that balance, channel and floodplain morphology adjust in response. On large regulated rivers, these pressures rarely act alone: flow regulation, sediment extraction, and urbanization act simultaneously and produce overlapping morphological signatures. Most studies attribute change to a single dominant driver or resolve change along a reach at one point in time, leaving the relative contribution of co-occurring drivers unresolved. Understanding which human drivers dominate that adjustment, and how their imprint varies along a river, is central to managing heavily used systems. This manuscript addresses the gap by integrating the temporal and spatial signatures of individual drivers to separate their contributions.

This study examines the geomorphic response of the Yamuna River to human activity, focusing on the heavily anthropogenically altered part of the river, spanning 460 km from the mountain front to the downstream of the Delhi megacity, making it an ideal system for disentangling competing controls on river morphology. We extracted the active floodplain from the Global Surface Water maximum-water-extent dataset (1984–2021) and delineated the corridor into 92 reach IDs, each 5 km long. For each reach ID, we quantified riverscape metrics, active channel width (ACW), water width (WW), braiding index (BI), and vegetation width (VGW), from Landsat and Sentinel-2 imagery spanning 1984–2024, and analyzed their change against the timeline of dam construction, sand mining, and urban expansion.

To isolate the effect of individual drivers, we divided the corridor into four segments defined by each driver's location, enabling before–and–after and upstream–downstream comparisons of their impacts. For each segment, we formulated hypotheses predicting expected river-scape changes, then tested and verified them against observed metrics. Human activity has measurably reshaped the riverscape, but the dominant control differs among drivers and along the river. At the segment scale, sediment mining emerges as the primary control on channel form, acting most strongly on active channel width and flow width. This reworking of the active channel decouples water width from discharge: across much of the studied reach, WW is no longer governed by flow but by mining-altered morphology, as reflected in the breakdown of the width–discharge relationship. Dam-driven flow regulation and urban expansion may have imposed secondary imprints superimposed on this mining signal, but they can't be detected. Together, these results show that, in intensively used alluvial rivers, direct sediment extraction can override hydrology as the first-order control on channel geometry, underscoring the need for informed, place-based management to preserve the ecological and geomorphic integrity of major Himalayan river systems amid intensifying anthropogenic pressure.

https://doi.org/10.5194/egusphere-2026-6100
Preprint. Discussion started: 11 November 2026
© Author(s) 2026. CC BY 4.0 License.

1. Introduction

Large rivers which attract over three billion people along their edges and encompass some of the world's most diverse ecosystems, serve as vital hubs for resources, agriculture, trade, and energy production (Best and Darby, 2020). They support populations that are often highly vulnerable to environmental and ecological stresses (Best and Darby, 2020). However, worldwide river ecosystems face multiple stressors, resulting in declining geo- and biodiversity, compromising ecosystem health and services (Tickner et al., 2020; Best, 2019; Peipoch et al., 2015; Vörösmarty et al., 2010; Dudgeon et al., 2006). Over two-thirds of the world's rivers are significantly impacted by anthropogenic activities (Giller,2005). Increasing population pressure and rapid urbanization have led to significant riverine degradation, further exacerbated by human activities and extreme weather events. Urbanization and population growth have been recognized as major drivers of changes in riverine landscapes (Chin, 2006; Meybeck, 2003). During the third quarter of the twentieth century alone, the global urban population increased by more than 100% and by nearly 200% in less-developed regions (Gupta, 1984). Walsh et al. (2005) introduced the term *"urban stream syndrome"* to describe the ecological degradation commonly observed in streams draining urbanized catchments. Large-scale water diversions pose additional threats to river survival (Ekka et al., 2020).

Channel morphological changes over the past centuries can be largely attributed to human-induced pressures, which have significantly impacted physical and biological processes (Downs and Gregory, 2014). Any changes due to natural and anthropogenic stresses in upstream flow, including changes in flood magnitude and frequency, or sediment regime (Best and Darby, 2020) may propagate through downstream reaches and be reflected in their forms and processes (Fryirs et al., 2007). As dams disrupt both water and sediment fluxes, they can have a major impact on river morphodynamics downstream, although the exact impacts will depend on the dam reservoir area and its operation, its location within a river basin, and the hydro-meteorological characteristics of the river itself (Church, 1995; Rollet et al., 2014). The factors associated with the downstream geomorphic effects of dams mostly orbit around the changes in the peak flow regime, as observed within the Great Plains (Friedman et al., 1998; Costigan andDaniels, 2012), inducing less energy downstream and favoring vegetation encroachment.

Dams can also trap bedload without significantly affecting flood regime (Rollet et al., 2014). Enhanced rate of progressive bed erosion is then observed downstream the dam that can also lead to channel narrowing propagation which is often associated with the riverward expansion of riparian vegetation into the downstream active channel (Friedman et al., 2022). Sediment mining is another significant anthropogenic activity that severely disrupts river geomorphology. As the second most consumed natural resource after water (Rentier and Cammeraat, 2022), sediment plays a critical role in modern construction. The rapid pace of urbanization and the demand for large-scale infrastructure projects have escalated the global need for construction materials, with sediment becoming an indispensable resource (Koehnken et al., 2020). Often referred to as "the new gold," the unregulated and excessive extraction of sediment has led to widespread degradation of physical and biological environments across the globe (Rentier and Cammeraat, 2022). Many of the world's rivers are extensively and frequently exploited as a natural resource for aggregate; 32 and 50 billion (10^9) tonnes of gravel and sand, respectively, are extracted from rivers globally each year (Quick et al., 2025). When undertaken at an industrial scale, aggregate mining often removes more material than a river can naturally replenish, creating a sediment deficit (Quick et al., 2025; Hackney et al., 2021). This deficiency is visible on morphological characteristics and leads to channel bed degradation, erosion of river bank,

https://doi.org/10.5194/egusphere-2026-6100
Preprint. Discussion started: 11 November 2026
© Author(s) 2026. CC BY 4.0 License.

thalweg shift and change in the planform of a river (Collins and Dunne, 1990, p.26). The removal of sediment through instream mining creates a sediment-starved condition, termed as hungry water (Kondolf, 1994, 1997), which forces a dual adjustment of the river morphology. Upstream of the extraction site, a local increase in energy and slope triggers regressive erosion through nickpoint migration (Galay, 1983; Rinaldi et al., 2005). Simultaneously, the trapping of bedload within the mining pit induces progressive erosion downstream, a process analogous to the geomorphic impacts of dams where the river compensates for its missing load by incising the channel bed and eroding banks to reach a new equilibrium (Church, 1995; Kondolf, 1994; Rollet et al., 2014).

Anthropogenic stressors rarely act in isolation, as river reaches are typically exposed to multiple, co-occurring pressures, and separating the relative effects of these stressors is essential for developing effective river management strategies (Lemm et al., 2021). As a result, multiple-stressor research has gained increasing attention across ecological subdisciplines, including terrestrial, marine, and freshwater ecology (Orr et al., 2020). It is established that environmental management measures addressing both anthropogenic and natural stressors cannot be effectively implemented without recognizing and disentangling their complex interactions (Dudgeon, 2019; Segurado et al., 2022; Lima et al., 2023). The first key challenge in multiple-stressor assessment is defining the spatio-temporal scope, which allows the hierarchy of stressors to be identified (Lima et al., 2023). Once this scope is established, hypotheses linked to individual stressors can be formulated to examine their cause–effect relationships. Cause-and-effect-based knowledge is crucial for evaluating the relative influence of human activities on river systems (Downs and Piégay, 2019).

One effective strategy for analyzing long-term river channel adjustments is to employ a multi-BACI (Before-AfterControl-Impact) approach (Kempton and Green, 1981), leveraging high temporal resolution information on planform adjustments. BACI approaches include time and impact factors, with a control site and a comparably impacted site, both represented by data before and after the impact (Seger et al., 2021). Early studies investigating river channel adjustments using airborne data relied on aerial photographs to reconstruct multi-temporal patterns of channel morphology and floodplain evolution, providing approximately a 40- to 50-year observational window (Geerling et al., 2006; Ollero, 2010; Segura-Beltrán and Sanchis-Ibor, 2013; Bollati et al., 2014; Arnaud et al., 2015; Clerici et al., 2015; Dufour et al., 2015; Lallias-Tacon et al., 2017). These studies demonstrated the effectiveness of multi-temporal aerial imagery for quantifying channel narrowing or widening, lateral migration, vegetation encroachment, and floodplain changes across diverse river systems, highlighting the value of remote sensing for long-term analysis of fluvial geomorphic changes and the tracking of the potential drivers based on the BA, CI, or BACI framework for inter-river and/or inter-reach comparisons.

With the emergence of new satellite-based archives, new opportunities to explore channel changes and their potential drivers have opened. Landsat archives provide a temporal window comparable to airborne datasets from the 1980s or 1990s when pioneer studies on channel changes emerged using aerial photo archives, spanning more than four to five decades, while offering substantially improved temporal sampling that enables multi-temporal and intra-annual pattern analysis (Henshaw et al., 2013; Wulder et al., 2019). A key technique to identify the geomorphic features from the multi-spectral images involves enhancing water-land contrast using indices such as the Normalized Difference Water Index (NDWI) (McFeeters, 1996), Modified Normalized Difference Water Index (MNDWI) (Xu, 2006), or Automated Water Extraction Index (AWEI) (Feyisa et al., 2014). Policy changes since 2008, coupled with the demand for a comprehensive GEE archive, have led to initiatives like the Landsat Global Archive Consolidation (LGAC) and

https://doi.org/10.5194/egusphere-2026-6100
Preprint. Discussion started: 11 November 2026
© Author(s) 2026. CC BY 4.0 License.

advancements in onboard systems and data transmission (Wulder et al., 2016). Such archives are particularly valuable for (1) large river systems (30 m spatial resolution) with dynamic planform changes, especially in alluvial systems of mountainous regions and their surroundings, where rivers have emerged bars and complex planforms, and (2) analyzing pressure chronologies over the past 40 years, ideally dividing data into pre- and post-20-year periods.

In this study, Landsat imagery spanning 1989–2024 is used to investigate morphodynamic changes along a 460-km reach of a Himalayan River and evaluate the relative contributions of multiple stressors and their role in shaping the observed morphodynamic adjustments, thereby providing insights relevant for informed river management. To achieve this, we formulated a set of hypotheses on cause-and-effect relationships and applied a BACI approach to validate them. We focus on the Yamuna main stem because it provides an ideal natural laboratory for examining human pressures using Landsat data. The major anthropogenic drivers affecting the river occurred during the study period (1984–2024) and show clear before-and-after sequences; their timing does not follow a single chronological pattern, and the scale of the riverscape is well-suited to Landsat-based analysis. This reach has been increasingly influenced by cumulative anthropogenic pressures, including flow regulation by an important dam (Hathinikund), extensive sediment extraction, and growing water abstraction associated with the expansion of a capital megacity. Rapid urbanization has intensified pressure on river systems, particularly in the wake of India's 1990s globalization. Delhi, the capital of India, exemplifies the severe impacts of unregulated urban growth, facing very high demand on water and sediment resources. Although the impacts of dams, mining, and land use or land cover changes in Delhi, on the Yamuna have been discussed in earlier studies (Bawa et al.,2014; Mittal et al., 2023; Yadav et al., 2023), their effects have not yet been quantified in an interlinked way using long-term, high-resolution spatial and temporal data, as proposed in the present work.

2. Study Area

The Yamuna River, the largest tributary of the Ganga River system in northern India, originates from the Yamunotri Glacier at an elevation of 6,387 m (Sharma et al.,2024). The river traverses a total distance of 1,376 km (Sharma et al.,2025) before merging with the Ganges at Allahabad in Uttar Pradesh, draining a basin area of about 3.46×10^5 km² (Joshi et al, 2022). Upstream of the study reach, the Yamuna flows through the Outer Lesser Himalaya with a gradient of about 0.5–0.6° (≈9–10 m km^{-1}; Patel et al., 2025). Downstream of the mountain front at Hathinikund, the mean gradient along the river corridor decreases to about 0.41 m km^{-1} over the 414 km to Vrindavan (derived from the DEM).

https://doi.org/10.5194/egusphere-2026-6100
Preprint. Discussion started: 11 November 2026
© Author(s) 2026. CC BY 4.0 License.

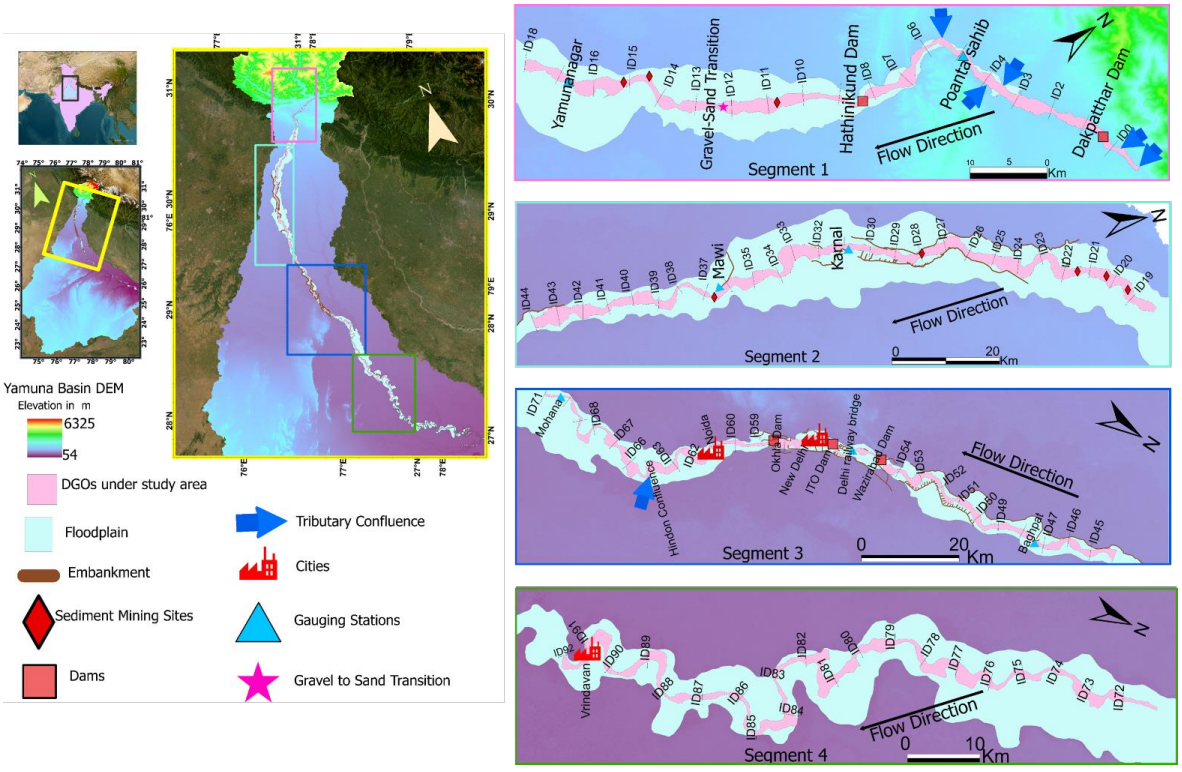


Figure.1: Study area Map of the Yamuna Basin from Upstream of the mountain front to the alluvial plain. The whole Study area is divided into four segments based on the presence of anthropogenic drivers. Segment 1 is marked by the presence of the Hathinikund dam, Segment 2 by the sediment mining activity, Segment 3 by the Delhi megacity, and Segment 4 is characterized by the downstream impacts of the Delhi megacity. The figure includes the gauging sites and major cities along with the tributary confluences. Each segment is further subdivided into 5 km-long river reaches, each composed of 10, 500 m-long DGOs (Disaggregated Geographic Objects). The DGOs serve as basic sampling units to extract landscape metrics, whereas the 5 km-long reaches represent the basic analysis unit. Elevation data: [SRTM DEM, NASA/USGS]. The satellite base map (World Imagery) was designed and developed by Esri | Powered by Esri; sources: Esri, Maxar, Earthstar Geographics, and the GIS User Community. For more information on this map, visit https://services.arcgisonline.com/ArcGIS/rest/services/World_Imagery/MapServer (last access: 11 November 2026).

The river is primarily rainfed, receiving most of its water from rainfall and groundwater, while glacial and snowmelt contribute only about 9% (Bookhagen and Burbank, 2010). At its confluence with the mighty Ganga River, the Yamuna River exhibits an annual discharge of approximately 96.1×10^9 m³ and transports a total sediment load of about 107×10^6 tons per year (Jha et al., 1988). The Yamuna River system has been broadly classified into 3 major channel reaches from the mountain front to its confluence with the Ganga River. It includes Natural reaches, Anthropogenically altered reaches, and Rejuvenated reaches (Bawa et al., 2014).

The present work is carried out on the 460 km length of the Yamuna River corridor, comprising the intermontane valley around Paonta Sahib (Bawa et al., 2014) to the mountain front around Hathinikund Barrage to the alluvial plains further downstream. The analysis includes the “Natural reaches” and “Anthropogenically altered reaches,” which are the first two classes after Bawa et al. (2014). In the study stretch, the basin is rainfed, and the river's perennial behavior is due to upstream storage and groundwater contributions as base flow (Rai et al., 2012).

https://doi.org/10.5194/egusphere-2026-6100
Preprint. Discussion started: 11 November 2026
© Author(s) 2026. CC BY 4.0 License.

This portion of the Yamuna River corridor is profoundly modified by anthropogenic pressures, such as dams (Table S1), notably Hathinikund dam built in 1999 (Mohanty and Tare, 2023) and operation started in 2002, with a 22,000 m^3 design flood capacity (Kumar et al.,2018); urbanization pressures, particularly those associated with the Delhi megacity; and sediment mining activities. The details of all the dams covered in the study area are described in Table S1 of the supplementary material.

Delhi, covering 1,483 km^2, is the world's second most populous city and the largest consumer of the Yamuna's water resources (Balha et al., 2020; Jha et al., 2026). Rapid urbanization, which increased the urban population from 0.21 million in 1901 to 16.37 million in 2011 (Sharma et al., 2022) and further 21.5 million in 2024 (Tanya et al., 2026), has placed severe stress on regional water availability. Further, between 2018 and 2030, Delhi is projected to record the highest absolute population increase of any city worldwide, adding around 870,000 inhabitants per year (UN DESA, 2019), highlighting rapid urban expansion and demographic pressure on the metropolitan region. Increasing population and urbanization have led to declining groundwater levels and reduced flows in the Yamuna River, which are now recognized as critical hydrological concerns (Chatterjee et al., 2009).

In addition to urban demands, sand and boulder mining, legalized for construction purposes, has emerged as a major driver of geomorphic and ecological change in the Yamuna River system. Sand and gravel mining is widespread along both the upstream and middle reaches of the study area, and in the foothill reach upstream of Hathinikund dam, it increased substantially after 2015 (Yadav et al., 2023). Intensive in-channel mining is known to cause groundwater depletion, accelerated bank erosion, and the loss of riparian ecosystems (Damseth et al., 2024). Although the permissible mining depth in the riverbed is limited to 3 m (Sinha et al., 2025), excessive and uncontrolled extraction has intensified these environmental impacts.

3. Materials and methods

3.1 Definition of the sampling units and raw data extraction from GEE

The approximate modern floodplain of the Yamuna River section was delineated using the Maximum Water Extent (MWE) layer from the Global Surface Water Explorer for the period 1984–2021, derived from Landsat archives (Pekel et al., 2016). This raster layer represents the maximum extent of detected water during that time frame. The MWE layer was extracted, vectorized, and cleaned by removing holes and anomalies based on morphological tools and on photo interpretation using satellite base maps available as WMS layers on QGIS. Secondly, we segmented the approximate modern floodplain into Disaggregated Geographical Objects (DGOs) with a length of 500 meters using the Fluvial Corridor Toolbox (FCT) (Roux et al., 2015). The length of the DGOs was chosen to closely follow the river bends shape while remaining short enough to provide a high level of detail for the river's features. This division spans from DGO 0 (Dak Patthar) DGO 920 (Vrindavan) (Fig. 1).

Different river metrics were extracted for all the DGOs. We used a new tool developed to leverage the Google Earth Engine (GEE) platform to extract riverscape metrics and indicators by calculating spectral indices for each DGO from all available Landsat satellite images during 1989–2024 (GloUrbEE; Dunesme et al., 2024). The GloUrbEE tool is built as a Python workflow that interacts with the GEE platform while taking advantage of the Python language and tools. The GloUrbEE workflow first allows calculation, for each DGO, of three common spectral indices from the Landsat archives: the Normalized Difference Vegetation Index (NDVI), the Normalized Difference Water Index (NDWI), and the Modified Normalized Difference Water Index (MNDWI) (Boothroyd et al., 2021).

https://doi.org/10.5194/egusphere-2026-6100
Preprint. Discussion started: 11 November 2026
© Author(s) 2026. CC BY 4.0 License.

These calculated indices were further used to extract three riverscape feature masks, namely the water, active channel (i.e., water and unvegetated sediment bars) and vegetation areas according to the following expressions: (1) water = 'MNDWI > 0.0'; (2) active channel = 'MNDWI > -0.4 and NDVI < 0.2'; (3) vegetation = 'NDVI > 0.15' (Dunesme et al., 2024; Yadav et al., 2023).

We obtained the masks for active channels, water and vegetation areas for each available image and each DGO. The workflow finally allows to vectorize the different masks and to calculate their surface areas (pixels) and perimeters (m). The workflow also provides mean values of the spectral indices at DGO and mask scales, as well as cloud and image coverage information for each DGO. The extracted metrics are exported for quantitative analysis. We retained for analysis only images with a cloud coverage below 20% and image coverage for each DGO of more than 90%.

3.2 Riverscape metrics and data analyses

Riverscape metrics such as water area, active channel area, and vegetation area were extracted for each DGO and scaled by multiplying by a unit pixel area of 900 m^2. Each resulting area was then normalized by dividing by the DGO_FID length of 500 meters to derive mean water width, mean vegetation width, and mean active channel width for each DGO. For the braiding index, half the water perimeter was divided by twice the DGO_FID width (1000 meters) to obtain the total sinuosity index for each DGO, following Hong and Davies (1979). Ten DGOs were grouped into a single reach unit to standardize the analysis, with the floor value assigned as the group ID. This approach resulted in 92 units called reach ID and each reach ID representing a 5 km-long river reach. Each reach ID has multiple observations per year, so to reduce the outliers and noise, median values of each parameter are taken for each year and

Reach ID. Image acquisition dates were decomposed into year, month, and day components for temporal analysis. R Studio (version 4.3.1) was used for data processing.

The final dataset contains all the median values by reach of variables recorded alongside date, month, and year. To assess temporal variations from 1989 to 2024, the calc_slope () function in R was employed to calculate the rate of change (slope) of the median value for each riverscape metric over time by ID. The resulting dataset includes reach IDs and the corresponding temporal slopes for each of the four riverscape indicators. Hence, each point in the downstream direction of a metric represents the slope of the trend line fitted with temporal data. Downstream variability of these slope values against reach IDs helps to visualize both temporal trends and spatial patterns in geomorphic changes. Further, a linear regression line was fitted for each riverscape parameter's slope values along river length to observe the downstream trend in overall data.

The consistency and reliability of the Landsat Archives, the number of observations available for each 5 km river reach, was analyzed and plotted (Fig. 2). This visualization allowed for the identification of temporal and spatial gaps within the dataset. It was observed that the period from 2004 to 2008 had the lowest data availability, indicating a significant reduction in the number of observations. Additionally, comparatively lower data coverage was observed for the earlier period from 1989 to 1993, suggesting potential limitations in data acquisition or satellite imagery availability during that time. Spatial inconsistencies were also identified, with reduced data density observed in specific river sections corresponding to reach IDs 58–66, 76–81, and 90–92 (Fig. 2). Understanding and accounting for these spatial and temporal variations in data availability is crucial for interpreting trends and ensuring the robustness of riverscape analysis across the entire study period.

https://doi.org/10.5194/egusphere-2026-6100
Preprint. Discussion started: 11 November 2026
© Author(s) 2026. CC BY 4.0 License.

Furthermore, following the River Styles framework (Brierley and Fryirs, 2000,2005), the Yamuna River has been classified into 13 distinct Geomorphic settings. This Geomorphic classification map was integrated with the riverscape metrics to assess the influence of underlying geology and geomorphic structure on the observed patterns.

The riverscape metrics were also compared with the hydrological variability. Hydrological data, including ten-daily discharge records and annual peak flow series, were obtained from the Central Water Commission (CWC) for multiple gauging stations along the river. These datasets formed the primary basis for formulating and testing the hypotheses developed in this study. The temporal coverage and continuity of the records, together with the reach ID of each gauging site, were systematically compiled and visualized in Fig. 3. Overall, the interplay between hydrology and geomorphology across the DGOs was analyzed.

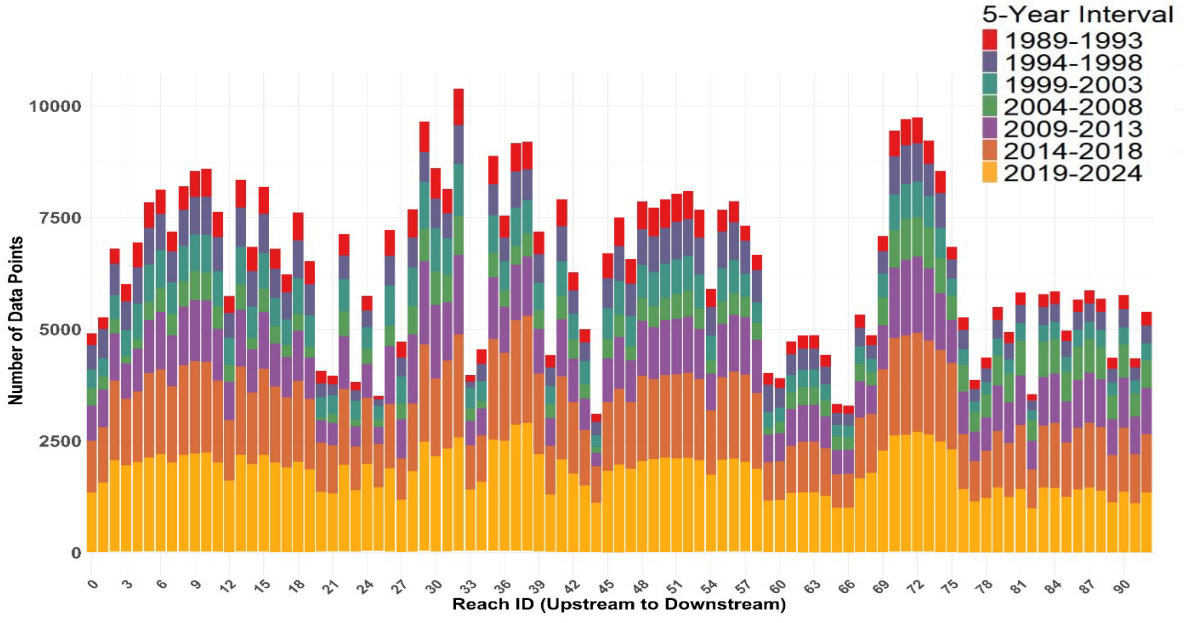
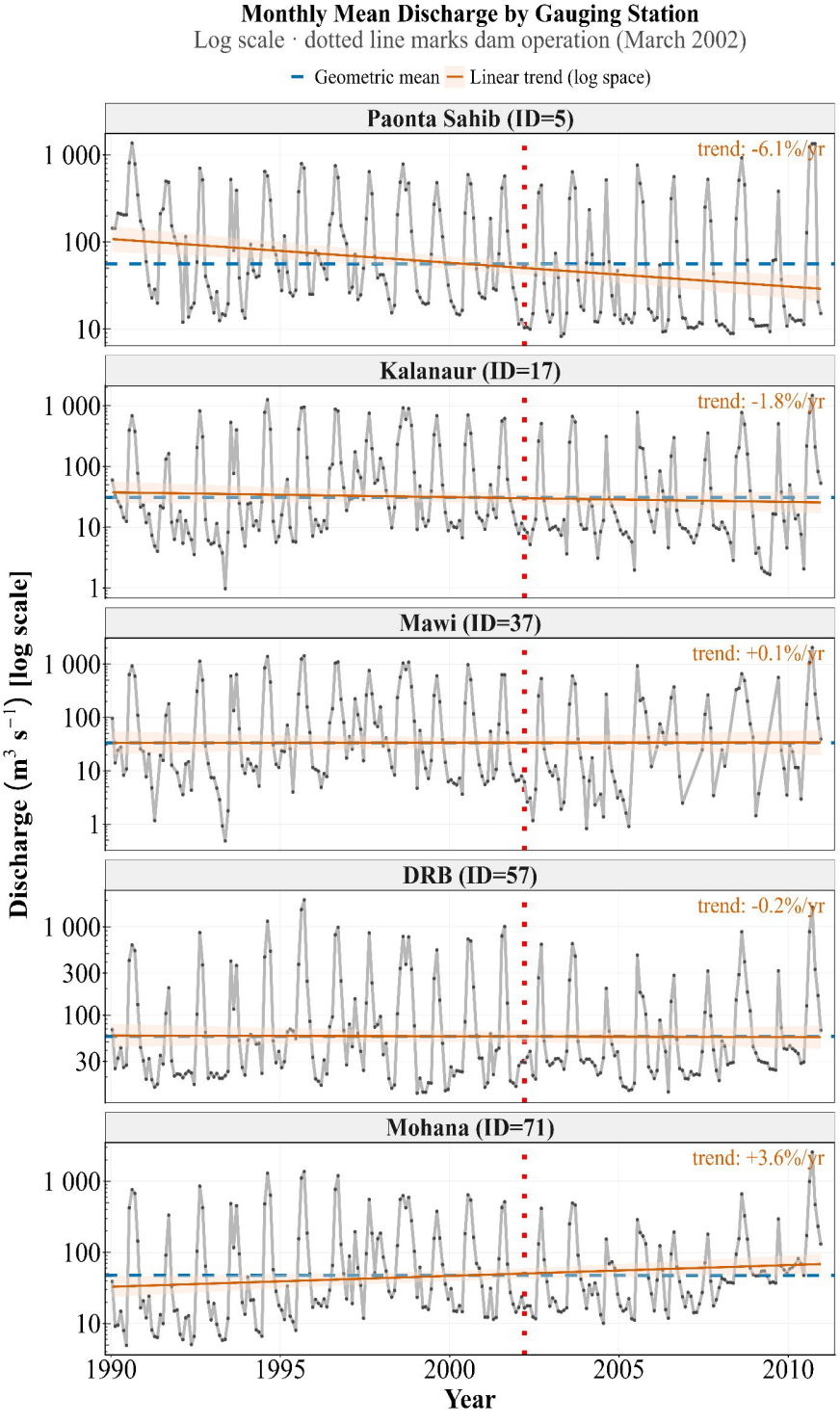


Figure 2. Landsat dataset availability across different years for each ID along the selected Yamuna River corridor.

https://doi.org/10.5194/egusphere-2026-6100
Preprint. Discussion started: 11 November 2026
© Author(s) 2026. CC BY 4.0 License.



https://doi.org/10.5194/egusphere-2026-6100
Preprint. Discussion started: 11 November 2026
© Author(s) 2026. CC BY 4.0 License.

Fig. 3 Ten-daily mean discharge values observed at 5 gauging stations along the selected Yamuna River corridor area. See Fig. 1 for locations of gauging stations. Gauging station Delhi Railway Bridge is marked as DRB. The solid orange line indicates the linear trend fitted to log10(Q), and the blue dashed line indicates the geometric mean. Trends are reported as percentage change per year.

3.3 Working hypotheses

Based on the different types of anthropogenic controls, we formulated six hypotheses to investigate the probable causes of riverscape geomorphic changes. The active channel width serves as a key metric for assessing the morphological dynamics of a river, representing the riverscape zone with flow channel and unvegetated bars (Bertrand et al., 2018). Therefore, in this study, we propose hypotheses using a hypothetico-deductive approach to identify the drivers influencing our study area through their cause–effect relationships, which vary across space and time.

Hypothesis H_0: In our first hypothesis we assume that there is no effect of anthropogenic disturbances on upstream controls (e.g., flood regiment and sediment delivery; Fig. 4(a) and Fig. 4(b)). This assertion is based on the assumption that if the controls were to have a substantial impact, discernible alterations would manifest in the active channel morphology (width narrowing with vegetation encroachment) in the most upstream segment (upstream Hathinikund dam; Fig. 1).

Hypothesis H_1: We assume here that the Hathinikund dam impacts the flood regime downstream. We then expect that channel narrowing (Fig.4(c) and Fig. 4(d)) is happening in the river across its entire course following the beginning of the Hathinikund dam activity (Construction begins in 1999 but it is operational in 2002). This conjecture is predicated on the notion that the activity of Hathinikund barrage induces a reduction in peak flow within the river system. Diminished peak flow, in turn, triggers a uniform narrowing phenomenon of equal magnitude throughout the river's length on a river section with no significant tributary. Our first segment from ID=0 to ID=18 is used to test this hypothesis having a B-A context (associated with the date of the dam construction, 1999; Fig.4(d)) and C-I context (associated with the dam location ID=9; Fig. 4(c)).

Hypothesis H_2: In this hypothesis, we assume that the sediment-starved conditions caused by Hathinikund dam activity led to a pronounced narrowing of the active channel width. This narrowing phenomenon arises due to sediment trapping by the dam, causing a reduction in the width of the active channel as sediment transport (Fig.4(e) and Fig.4(f)) and deposition becomes limited. This narrowing in the active channel width depends first on the distance from the dam, and then on time as it propagates downstream. It occurred earlier near the dam and later on downstream signing a propagation of change. We use here again our first segment from ID=0 to ID=18 to test this hypothesis but we expect a space-time active channel width adjustment, a different from H_1.

Hypothesis H_3: We assume mining pits exist all along the reach from ID=19 to ID=44 and the intensity of sand mining is the same throughout the course of the river. Thus, the uniform intensity of sand mining contributes to a consistent pattern of active channel width alterations along the river, the narrowing being associated with the incision and starvation due to mining. If mining sites do not have the same intensity, local maximum narrowing can be variable. In the beginning of the mining period we observe a uniformly wide channel along the segment. And in the period when the mining started, we expect cyclic alteration in the active channel width with incision and recovery. However, we

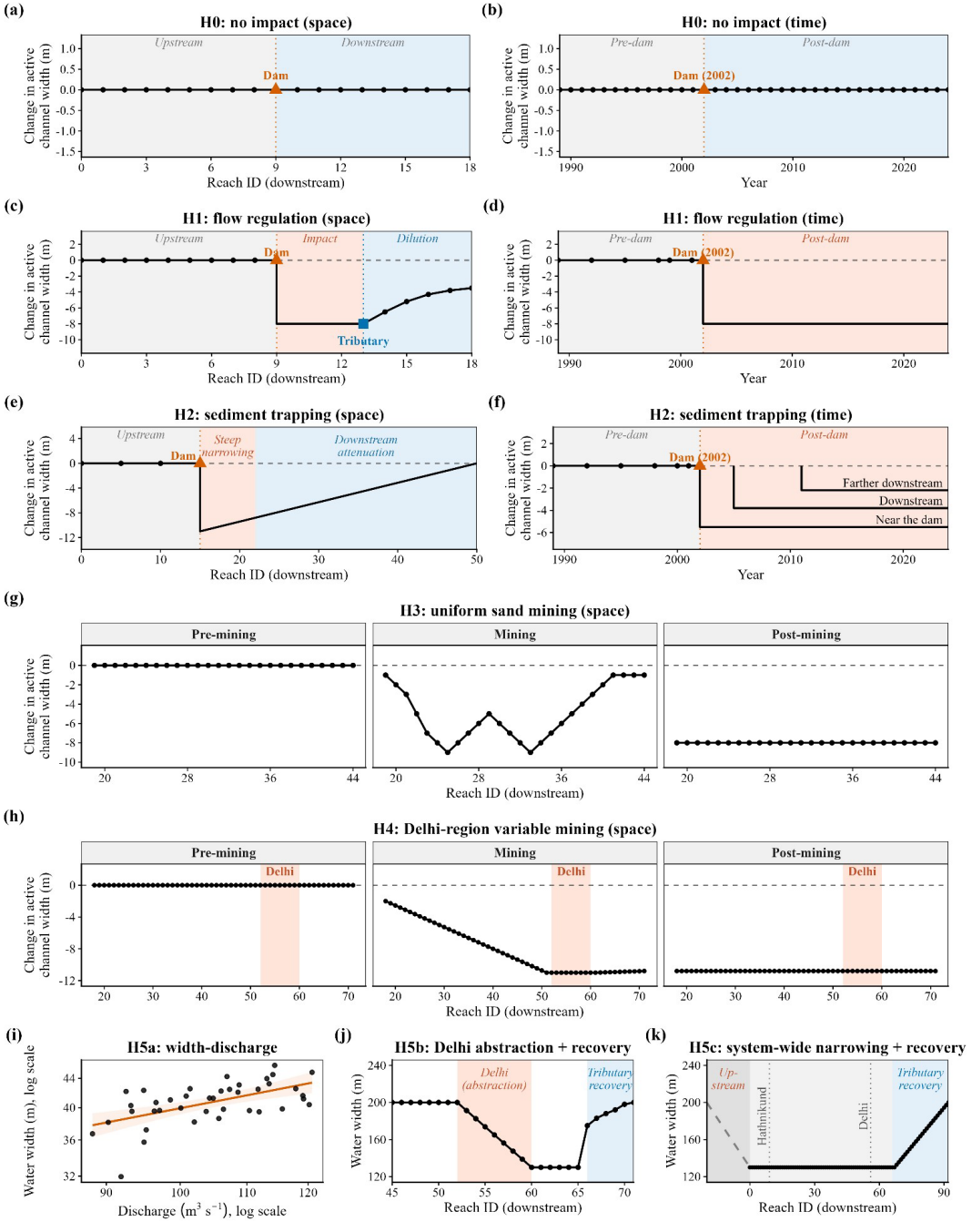
https://doi.org/10.5194/egusphere-2026-6100
Preprint. Discussion started: 11 November 2026
© Author(s) 2026. CC BY 4.0 License.

expect a narrowing everywhere along the segment in the current time period because of regressive and progressive erosion upstream and downstream of each mining site (Fig.4(g)).

Hypothesis H_4: In this hypothesis, we expect that the impact of mining activities extends throughout the entirety of the river, but is particularly pronounced close to the Delhi region. This assertion suggests that mining activities exert varying degrees of influence along the river's course, with the highest intensity occurring in the vicinity of Delhi (Fig. 4(h)). Under this premise, we anticipate observing more substantial alterations in the active channel width within the Delhi region compared to other sections of the river, according to urban development. Our third segment from ID=45 to ID=71 is defined by the presence of Delhi megacity (Fig.1). In this hypothesis which is tested in the reach ID=18 to reach ID=71, we expect the same temporal scenarios as of Hypothesis $H_{3\ but}$ a higher intense narrowing in the Delhi region (Fig.4(h)).

Hypothesis H_5: In this hypothesis we analyse the relationship between hydrology (the mean 10 days' discharge) and water width in three different scenarios. Through this hypothesis we aim at demonstrating that the water width is not only linked to discharge but also to morphological changes: if through time 10-days discharge does not change and water width changes, it means geomorphic pattern changes are dominant over hydrological processes, as the channel flow width does not accommodate the changes in flow following the classic hydraulic formulae W=aQ^b (Morel et al. 2019). In the first scene of analysis we expect that, with no hydrological changes, with a potential increase in the discharge, there will be an increase in the water width (Fig.4(i)). This part of the hypothesis will be tested on the reach IDs for which discharge data is available and this relationship to hold true for all the gauging stations. In the second scenario (Fig.4(j)) we expect a sharp decrease in the water width in the Delhi region which is linked to the water abstraction activity there. If flow derivation from Hathinikund is significant, the same pattern can be observed but then in the downstream of the Hathinikund dam also after its operation in 2002. This narrowing propagates downstream until the effect is smoothed by a significant tributary contribution. In the last part of the hypothesis (Fig.4(k)) we analyse the impact of an upstream control (e.g., changes in basin contribution) on water width, where the water width is narrowing everywhere in the segment and the impact is getting smoothed with a tributary confluence. It then occurs upstream and downstream of Delhi or Hathinikund dam and without any link with the chronology of their pressure.

https://doi.org/10.5194/egusphere-2026-6100
Preprint. Discussion started: 11 November 2026
© Author(s) 2026. CC BY 4.0 License.



282

283 **Figure. 4 Conceptual plots for different hypotheses of anthropogenic impacts on river channel morphology,** 284 **especially channel width variation.**

https://doi.org/10.5194/egusphere-2026-6100
Preprint. Discussion started: 11 November 2026
© Author(s) 2026. CC BY 4.0 License.

5. Results

5.1 Longitudinal pattern of temporal trends of riverscape metrics

Temporal trend of each riverscape metric was analysed through scatter plots from 1984 to 2024 for each of the reach ID (Fig. 6-8, Fig. S1 to S8 of Supplementary material). Each slope values (y-axis) on Fig. 5 for any reach ID represent temporal trend of the corresponding metric for that specific reach ID. Hence, negative values indicate a declining temporal trend in the corresponding riverscape metric for that reach ID, whereas positive values reflect an increasing trend over time, representing the average temporal variability of that parameter at specific reach ID locations. Temporal trend per reach along channel length was assessed using four primary riverscape metrics: Active Channel Width (ACW), Braiding Index (BI), Vegetation Width (VGW), and Water Width (WW) (Fig. 5). Geomorphic variability along long profile was represented through various parameters following the framework of the River Styles classification (Brierley and Fryirs, 2000,2005). The study reach of the Yamuna River is characterized by four distinct geomorphic settings. Each setting was delineated on the basis of valley setting, channel planform, and the arrangement of instream and floodplain geomorphic units, allowing the river to be partitioned into internally consistent reaches of comparable process–form behaviour.

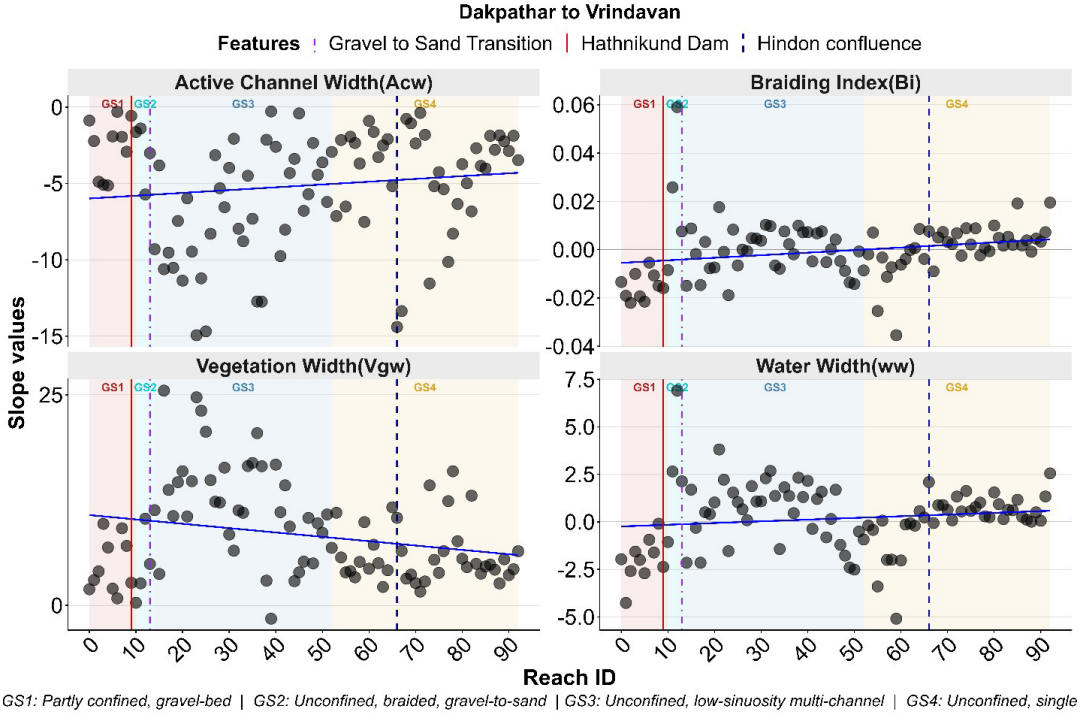


Figure 5: Variability of riverscape metrics across the overall study area of the Yamuna River. Geomorphic Settings (GS) channel reaches have been marked along Reach IDs. Each reach ID represents a 5 km river length and each point in the plot represents the regression slope of temporal trend of the reach from 1984 to 2024, according to Fig. 6-8 and S1-S8. The figure depicts the spatial variation of temporal slope values of each reach ID.

https://doi.org/10.5194/egusphere-2026-6100
Preprint. Discussion started: 11 November 2026
© Author(s) 2026. CC BY 4.0 License.

Throughout the study area, the active channel width is consistently negative, indicating channel narrowing across all reach IDs from 1989 to 2024. Slope values range from 0 to -15, with the lowest slope observed in ID=24 (Fig. 5). A slight increase in the overall trend suggests the narrowing is more pronounced in the upstream part of the study reach than in the downstream. The vegetation width is always positive, with a downstream-declining trend, indicating encroachment reduction in downstream reaches. Slope values vary from -1.58 to 25.50, with the only negative slope observed in the ID=39 (Fig. 5). Vegetation width shows an inverse relationship with active channel width, confirming that active channel narrowing is linked to a channel adjustment associated with vegetation encroachment. Four main spatio-temporal trends are then observed:

Reaches ID 0 to 9 display almost no active channel narrowing and no vegetation encroachment, potentially confirming H0. This means that upstream controls (sediment supply and flood regime) are in a fairly steady state over the period for these reaches.

Reaches ID 10 to 40 show the most important transformations with maximum active channel narrowing and vegetation encroachment.

Reaches ID 40 to 70 display slighter narrowing of active channel and vegetation encroachment with a higher local variability than reaches 0 to 9.

Reaches ID 70 and downstream reaches show a trend close to upstream reaches (0-9).

The water width shows a fluctuating trend with negative values in the upstream mountainous region and Delhi region and positive slopes nearly everywhere else (Fig. 5). The slope values range from -5.10 to 6.90, with the most negative value observed in ID=59 (Fig. 5). The Braiding Index follows a trend similar to that of water width. The slope values range from -0.03 to 0.06 with the most negative value observed in the ID=59 (Fig. 5). These two metrics also confirm the four main longitudinal trends identified above.

From the preliminary results, it was observed that H_1 and H_2 (flow regulation and sediment trapping by dam) are not validated, whereas H_3 and H_4 needed a deeper analysis from the raw results provided by individual temporal trends at reach ID scale, where H_3 seems more probable than H_4 because most of the channel changes occur far upstream Delhi rather than close to it. However, the longitudinal trend as a whole is complex, confirming longitudinal water width is disrupted by channel adjustments that potentially modify the channel pattern geometry, as the BI index shows a linked pattern with the WW trend.

5.2 Variation of riverscape metric with discharge changes

Hydraulic geometric equation after Leopold and Maddock ,1953 was used to analyze the dependence of wetted width on hydrological change. Width and discharge are related through a power function (Eq.1):

$$W = aQ^b \quad (1)$$

where W is the wetted width of the channel, Q is discharge, a is a coefficient, and b is the width exponent describing the sensitivity of width to changes in flow. The yearly median of water width was compared against the yearly median of the ten-daily discharge at each gauging site, and both variables were log10 transformed so that the power relationship reduces to a straight line whose slope yields the exponent b (Fig. 6).

Because the relationship was derived from interannual variation at fixed gauging sites, the resulting exponents describe *at-a-station* hydraulic geometry and suggest how a given reach adjusts its width to year-to-year changes in discharge rather

https://doi.org/10.5194/egusphere-2026-6100
Preprint. Discussion started: 11 November 2026
© Author(s) 2026. CC BY 4.0 License.

than the downstream progression of width along the river. At-a-station width exponents ranged from 0.21 to 0.67 (Fig. 6). Values varied non-monotonically in the downstream direction, with the highest exponent at Mawi (ID = 37) and the lowest at DRB (ID = 57). The high exponent at Mawi indicates a reach whose width adjusts readily to changes in flow. In contrast, the low exponent at DRB indicates a reach whose width is comparatively insensitive to discharge. The channel in this reach is anthropogenically confined through embankments, which may have weakened the coupling between discharge and channel form.

The absence of a systematic downstream trend in b suggests that width adjustment is governed by local reach conditions rather than by discharge alone. These exponents were therefore examined further in the context of Hypothesis H5a through a segment-level analysis, to establish whether the reach-scale variability in width–discharge coupling reflects flow regulation, sediment dynamics, or sediment mining.

https://doi.org/10.5194/egusphere-2026-6100
Preprint. Discussion started: 11 November 2026
© Author(s) 2026. CC BY 4.0 License.

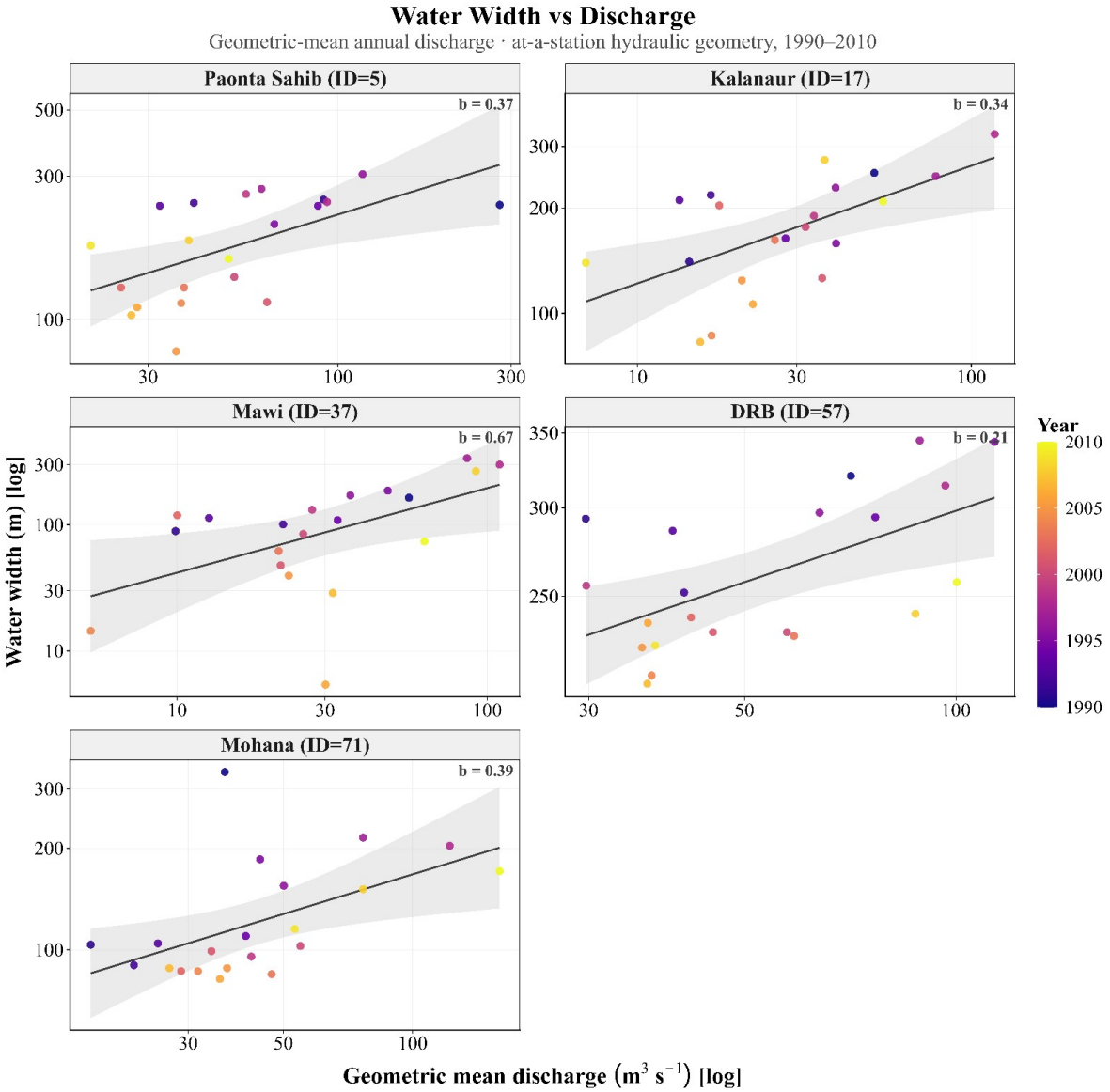


Figure. 6 Variation of Water width at a gauging site with the change in discharge values at that site. Both the WW and Discharge values are in logarithmic form.

5.3 Riverscape metric patterns in the four main spatio-temporal segments

The BACI approach was used for the detailed analysis to interpret and discuss the results on the four main spatiotemporal trends observed. For this purpose, reaches are grouped into four main segments.

https://doi.org/10.5194/egusphere-2026-6100
Preprint. Discussion started: 11 November 2026
© Author(s) 2026. CC BY 4.0 License.

5.3.1 Segment-1: Hathinikund dam dominated reaches

We took a 90 km river segment from ID=0 to ID=18 to better assess Hypotheses H_0, H_1, and H_2. These hypotheses were used to analyze the effect of Hathinikund dam (Hd) on the spatial variation in riverscape parameters (Fig. 7a and b). This river segment was chosen deliberately to see the impact 45 km upstream and 45 km downstream of Hd which is located at ID=9 (Fig. 1).

Annual median values of active channel width (ACW) were plotted for each 5-km reach ID to evaluate temporal trends for each reach ID and assess potential riverscape responses to dam activity after 2002 (Fig. 7a). The observed variability indicates that Hypothesis H_0 (no significant riverscape change upstream the dam) does not fully hold, as pronounced changes in ACW (Fig. 7a) are evident in both upstream and downstream sections. The upstream reaches underwent abrupt channel narrowing on different dates, sometimes before, sometimes after, sometimes at the same time as the beginning of dam activity. ACW decline ranges between approximately 50 and 200 m over the study period. The shift is mostly abrupt but with a distinct chronology from one reach ID to another: 2002 for ID1 and 2, 2008 for ID 4, 2012 for ID 0, ID 14 or ID 5, possibly sooner than 2002 for ID8 (i.e., no clear trend for all the DGO but local adjustments).

To examine the potential influence of the Hathinikund dam (Hd), its year of operation (2002) was used as a temporal breakpoint to distinguish pre- and post-operation trends. Compared with the upstream reaches, the downstream reaches show a similar pattern but a steeper decline. Notably, in most reaches the onset of pronounced narrowing occurs around 2011–2013 rather than immediately following the start of dam operation. This delayed and spatially localized timing indicates that channel change is driven by local perturbations with their own chronology, independent of the dam: the changes appear too late, and lack the progressive downstream-attenuating signature that dam-induced sediment starvation would produce under H_2 and H_3 hypothesis. We therefore find no evidence that the dam is a primary control on the observed channel changes.

Vegetation width (VGW) displays an inverse relationship with ACW, showing consistent increases in both upstream and downstream reaches, and across both pre- and post-construction periods (Fig. S1, Supplementary Material). The rate of vegetation expansion is more pronounced in sandy-bedded reaches compared to gravel-bedded reaches (Fig. S1, Supplementary Material).

Water width (WW) exhibits a distinct pattern upstream and downstream of the Hathinikund dam (Fig. 7b). In upstream reaches, WW decreases markedly through the period. Fig. 6 shows that, for ID 5, the WW-Q relationships change over time, with WW decreasing for a given discharge. Together, these observations indicate that WW reflects a change in the channel geometry. In the downstream reaches of the dam, WW exhibits an inconsistent trend, with fluctuating yearly median values (Fig. 7b). Notable exceptions are observed at IDs 11, 12, and 13, where WW shows an increasing trend despite the overall downstream decline. This reach corresponds to the gravel-to-sand transition (ID = 13) and is characterized by a laterally unconfined braided planform extending from ID 10 to ID 14. Fig. 6 shows the WW-Q relationship for ID17. Similarly, to ID5, we observe here a shift in the WW-Q relationships, with WW decreasing over time for a given discharge. Field observations and high-resolution imagery confirm the presence of extensive stonecrusher operations and active in-stream sediment-mining patches along these reaches. Examination of the Landsat time series reveals that the original multi-thread braided pattern, comprising numerous narrow, widely distributed branches, progressively transitions to fewer, wider, and more consolidated water channels in the mined reaches (Fig. S11). These

https://doi.org/10.5194/egusphere-2026-6100
Preprint. Discussion started: 11 November 2026
© Author(s) 2026. CC BY 4.0 License.

consolidated channels are more consistently detected at the 30 m pixel resolution of Landsat, whereas the pre-existing narrow individual threads frequently fell below the detection limit. The resulting increase in WW at IDs 11–13, therefore, reflects a change in channel planform configuration rather than an increase in discharge.

The Braiding Index (BI) follows a pattern similar to water width, with an overall decline in braiding intensity after barrage construction (Fig. S5, Supplementary Material).

The temporal sequence of ACW changes was examined to evaluate Hypotheses H_1 and H_2, where we expect channel narrowing following dam activity and its downstream propagation. Although channel narrowing is observed in downstream reaches, the timing of contraction does not correspond with the 2002 dam operation year. Several structural breaks in channel width are identified (Fig. S9, Supplementary Material), with the most prominent occurring around 2011–2012. This period coincides with intensified gravel extraction activities near IDs 0, 3, 6, 10–14, where multiple stone-crushing sites are also visible downstream of the dam in Landsat imagery from 2011 onward. Stone crushing sites were also observed during the field visits in October 2022, as mentioned earlier, further validating the ongoing sediment mining activities in the reach both downstream and upstream.

Additionally, within this river section (IDs 10–14), the river transitions from a highly braided morphology (Geomorphic Setting GS2; Fig. 5) to a predominantly single-thread channel during the same temporal window (Fig. S11, Supp.Mat.), indicating substantial planform simplification in response to gravel extraction but not because of the dam effect. A detailed analysis of 5 km by 5 km windows shows that H_0, H_1, and H_2 are not validated, suggesting upstream drivers (H_0) but also potentially other local drivers.

https://doi.org/10.5194/egusphere-2026-6100
Preprint. Discussion started: 11 November 2026
© Author(s) 2026. CC BY 4.0 License.

416

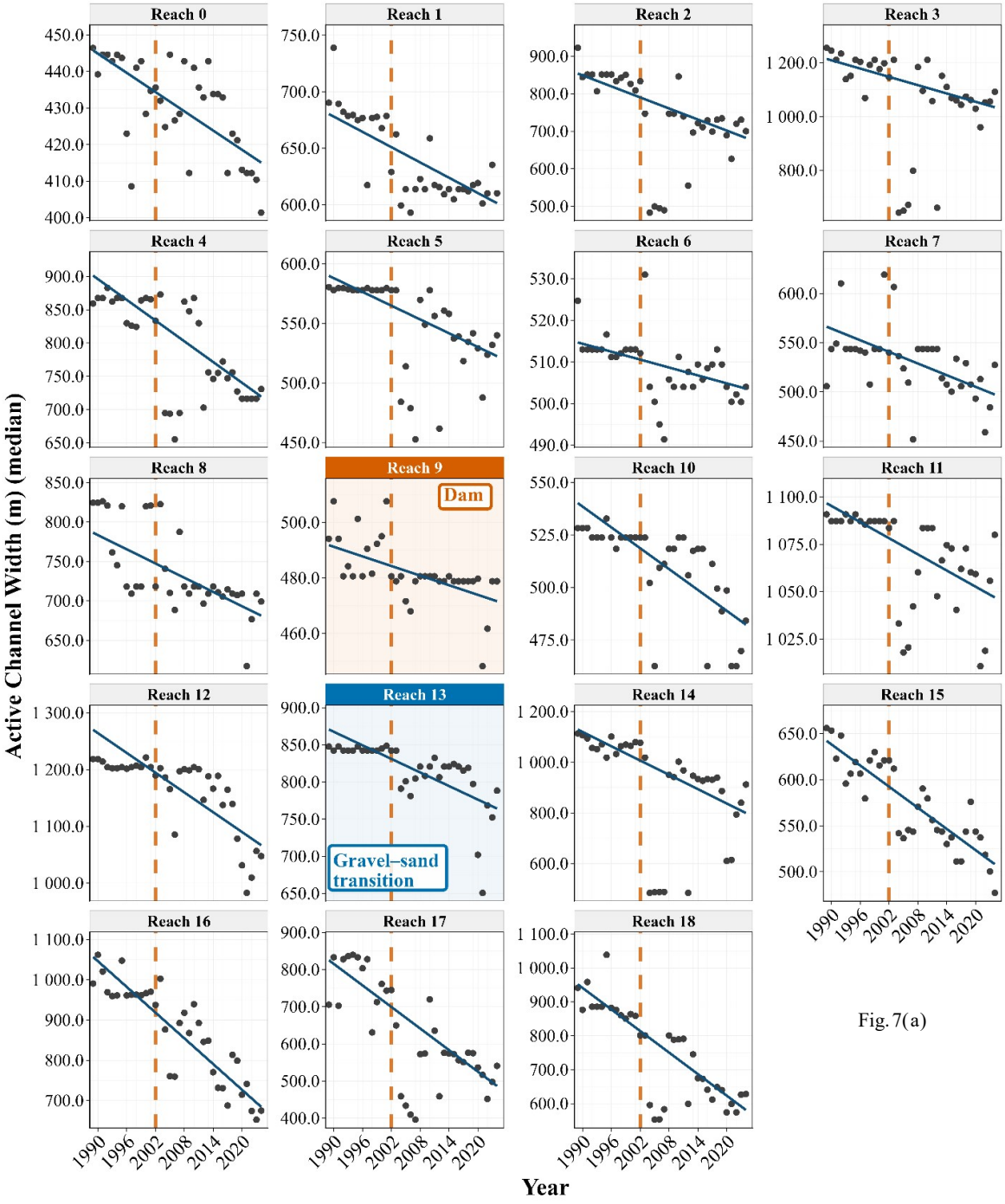


Fig. 7(a)

https://doi.org/10.5194/egusphere-2026-6100
Preprint. Discussion started: 11 November 2026
© Author(s) 2026. CC BY 4.0 License.

417

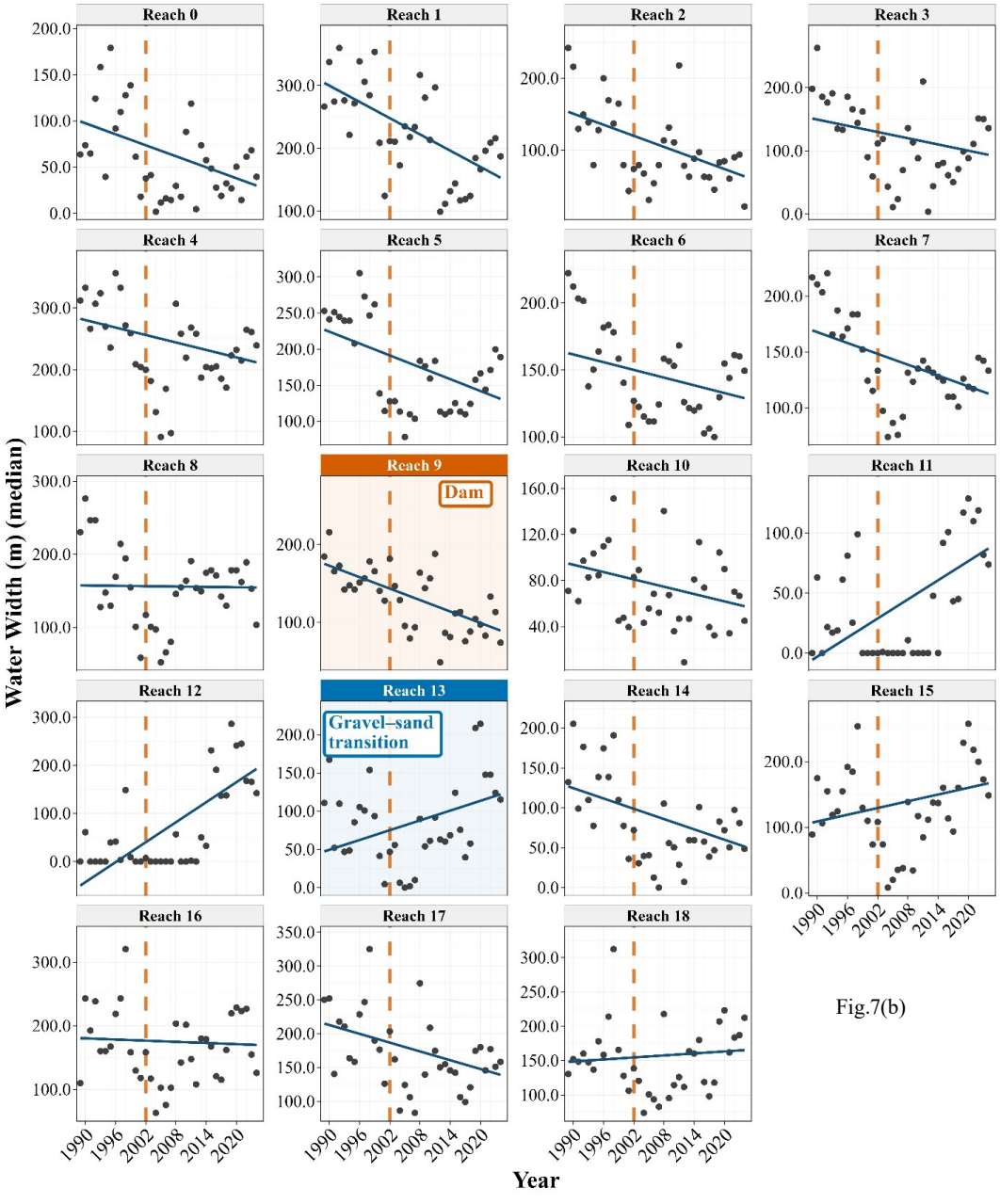


Fig.7(b)

418 **Figure. 7. Variation of yearly median active channel width (a) and yearly median water width (b) along the** 419 **Segment 1 from Reach ID 0 to Reach ID=18. The orange dashed line indicates the year of dam operation (2002).**
420 **Dam is located at reach ID 9 and reach ID 13 is marked by the transition of grain size from Gravel to Sand.**

https://doi.org/10.5194/egusphere-2026-6100
Preprint. Discussion started: 11 November 2026
© Author(s) 2026. CC BY 4.0 License.

5.3.2 Segment-2: Sediment mining dominated reaches

Although sediment mining occurs throughout the entire study area, this 75-km segment (from ID 19 to ID 44; Fig. 5) exhibits particularly intensive extraction and represents a distinct geomorphic control zone along the Yamuna River. Satellite observations indicate marked increases in mining activity during 2011, 2015, and 2021 (Yadav et al., 2023) which were verified in the field. This segment was tested against the hypothesis H_3 to see the impact of uniform intense sediment mining. The segment is characterized by a laterally unconfined, low-sinuosity, multi-channel morphology, within which large-scale sediment extraction is visible along much of the channel corridor. Extraction sites were identified through satellite imagery, documented reports, and field observations. Prominent mining locations occur at Pobari (ID 20), Jathalana (ID 20), Gumthala (ID 21), Chogawan (ID 22), Gadpur (ID 23), Alipura (ID 26), Bazidpur (ID 28), Shamli (ID 30), Karnal (ID 32), Mawi (ID 37), and Mamaur Ahatmali Hall (ID 38), also visible in Fig.S14.
This segment shows a persistent trend of active channel narrowing, with rates of contraction steeper than those observed in upstream reaches (Fig. 8a). In addition to long-term narrowing, active channel width (ACW) exhibits pronounced cyclical fluctuations. Vegetation width (VGW) displays a corresponding increasing trend with superimposed cyclic variation (Fig. S1-Fig. S4 Supplementary Material). In contrast, water width (WW) shows an overall increasing trend throughout the reach (Fig. 8b), and a similar pattern is observed in the braiding index (BI) (Fig. S6 Supplementary Material).
The temporal behavior of ACW in this segment is characterized by consistent narrowing combined with oscillatory fluctuations (Fig. 8a). It aligns with the expectations of hypothesis H_3, which anticipates relatively uniform mining intensity across the reach and a zig-zag pattern in channel width response. Analysis of the dataset, excluding the anomalous period of 2004–2008, reveals distinct morphodynamic behaviors across two temporal phases. During premining time (before 2014-2013), a uniformly wide channel is observed, and during mining, a cyclic pattern is observed, with narrowing in recent times (Fig. 8(a)), satisfying hypothesis H_3. VGW (Fig. S2) shows an inverse relationship with ACW, with an increasing trend across all reaches of the segment.
The temporal behavior of WW (Fig. 8(b)) suggests an increasing trend, except for the inconsistent period of 20042008, which can be linked to the mining pit captured by the channel, as the increase began after ~2014. BI's temporal behavior was similar to that of WW, suggesting an interdependency again. Fig. 6 presents a WW-Q relationship for ID37 that shows trends similar to those observed on ID5 and ID17, demonstrating the impact of geomorphic changes and validating H5a.

https://doi.org/10.5194/egusphere-2026-6100
Preprint. Discussion started: 11 November 2026
© Author(s) 2026. CC BY 4.0 License.

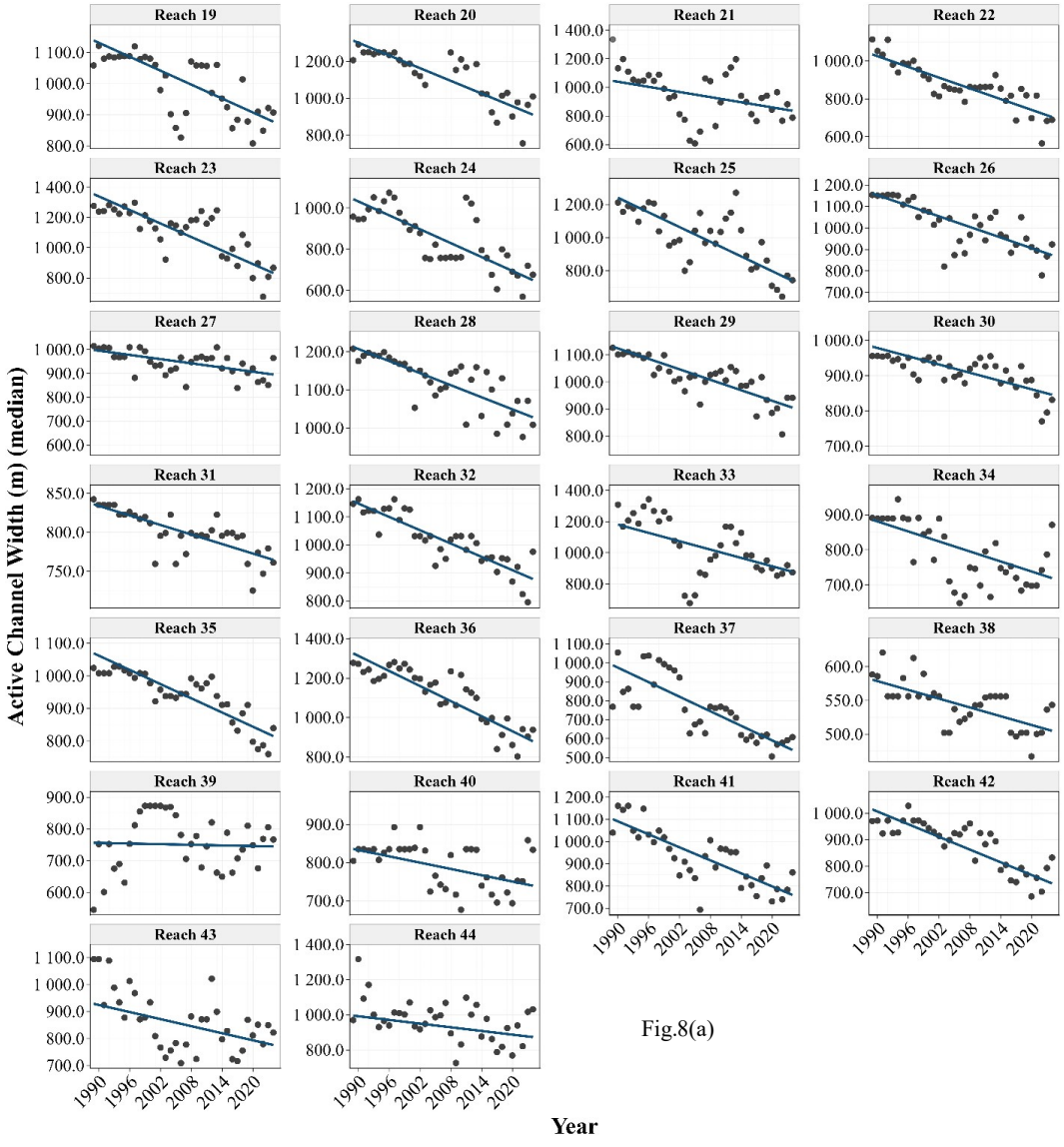


Fig.8(a)

https://doi.org/10.5194/egusphere-2026-6100
Preprint. Discussion started: 11 November 2026
© Author(s) 2026. CC BY 4.0 License.

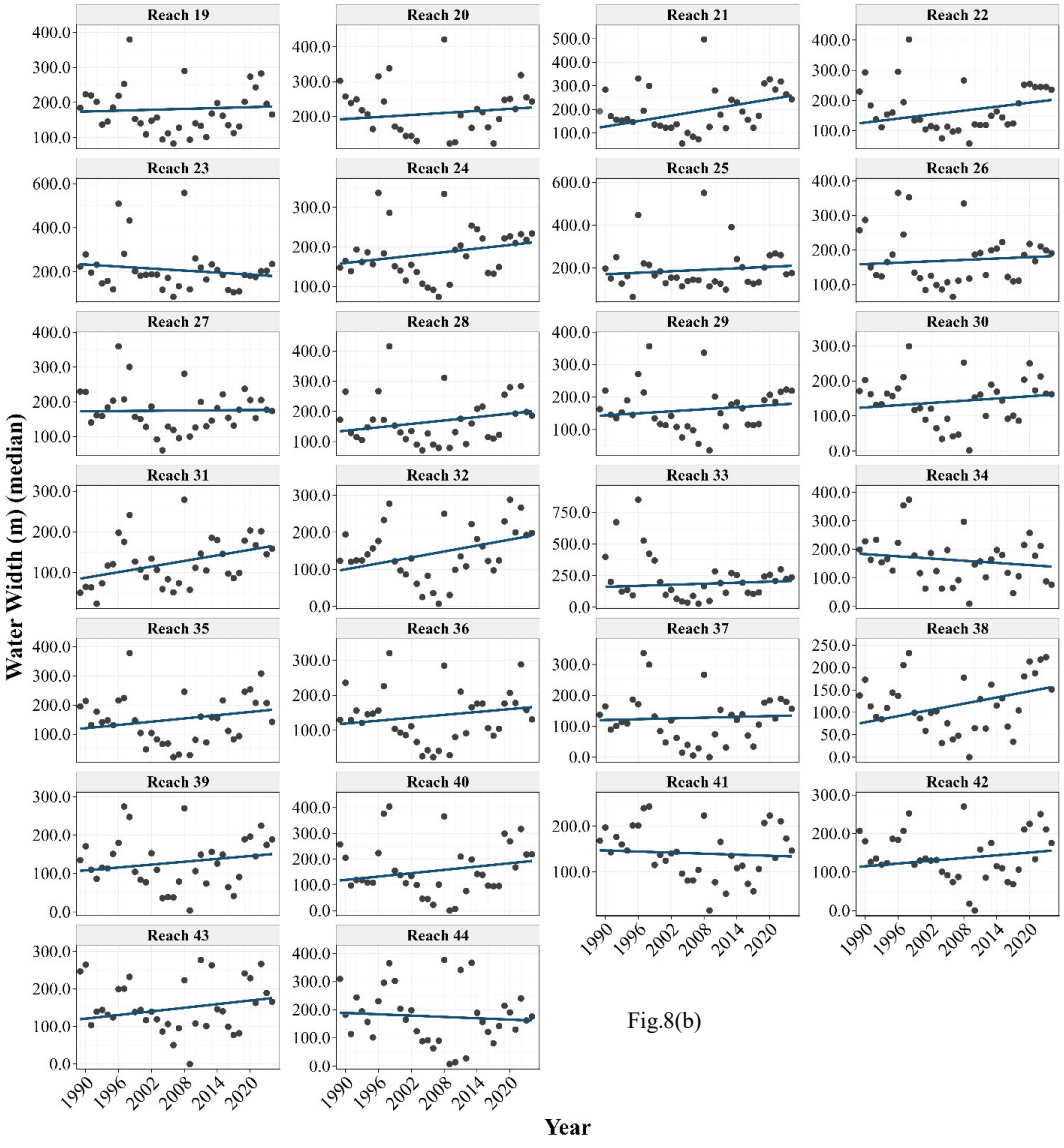


Fig.8(b)

Figure .8 (a)Variation of yearly median active channel width along the Segment 2 from Reach ID = 19 to Reach ID=44 and (b) Variation of yearly median Water width along the Segment 2 from Reach ID = 19 to Reach ID=44

5.3.3 Segment-3: Reaches in the proximity of Delhi Megacity

The influence of the Delhi metropolitan region on channel morphology was evaluated along a 130-km segment of the Yamuna River, comprising a 35-km upstream reach (IDs 45-53), a 40-km urban corridor (Delhi section; IDs 52-60), and a 55-km downstream reach (IDs 61-71; Fig. 9a). The upstream boundary of the urbanized zone is marked at Palla (ID = 52), while the downstream limit corresponds to the Okhla Barrage (ID = 60) (Fig. 1).

https://doi.org/10.5194/egusphere-2026-6100
Preprint. Discussion started: 11 November 2026
© Author(s) 2026. CC BY 4.0 License.

A clear downstream transition in channel morphology is observed within this segment. The upstream reaches are characterized as a laterally unconfined, low-sinuosity, multi-channel style, whereas the Delhi segment and its downstream continuation transition into a laterally unconfined, moderate-sinuosity, single-channel system (Fig. 9a). Throughout this stretch, the channel is strongly embanked and flow is regulated by multiple barrages (Figs. 1 and 9a). Additionally, the Yamuna River is joined by its tributary Hindon River at ID = 66 (Figs. 1 and 9a), introducing an additional hydrological input in the downstream section.

Sand mining activity is particularly prominent in the upstream part of this segment, especially near Bakhtawarpur (ID 46) and Asadpur (ID 48). A consistent trend of channel narrowing is observed across the entire 130-km reach (Fig. 9a). Vegetation width exhibits a steady increasing trend with comparatively moderate slopes (Fig. S3, Suppl. Material). We observed abrupt or more continuous decline, with a local maximum with temporal patterns very similar to the reach immediately upstream but less intense, demonstrating H_4 is not validated and H_3 is much more consistent, mining acting in the largest upper sections with a high sediment resources accessibility and availability in a wider braided reach than the one near Delhi.

Water width (Fig. 9b) shows greater variability, with most reaches showing a decreasing trend, sometimes abrupt (IDs 48, 49, 50, 51, 54, 57, 58, 59, 65). Temporal trends suggest that the early 2000s serve as the main breakpoint for Reach IDs upstream of the Delhi Region (Fig. 9 b), specifically for IDs 45-65. This chronology matches both the mining and dam operations in 2002, but the distance-decaying character of the dam impact potentially indicates the influence of overall mining pressure on channel geometry and again validates the H_3 hypothesis. The impact of Delhi megacity and its water abstraction is not visible on the reaches in the downstream of Delhi region (ID=60) with median values fairly steady-state at the range of ~100-150m in the reaches after that, with a slight water width increase after ID=64 (see ID 65, ID 68, ID 67, ID 69), some of them showing also the early 2000 shift earlier (ID 64 or ID 65). This reach does not satisfy the Hypothesis H_{5b}, suggesting the Delhi water abstraction theory and tributary impact as the recovery predicted under H_{5b} is confined to the Hindon confluence reach (ID 66) alone, where width rises from approximately 120 m to 230 m. This increase does not propagate: adjacent downstream reaches remain flat despite the additional tributary discharge. The at-a-station relations (Fig. 6) point to the same result from the other direction at ID 57 and ID 71, width at a given discharge declines through the record (Fig.3), and the width exponent at ID 57 ($b = 0.21$) is at the low end of reported at-a-station values. Width, in other words, is no longer adjusting to discharge in this reach. The apparent inconsistency at ID 71, which is temporally flat in Fig. 9b yet declining in Fig. 6, follows directly: discharge increased after the tributary confluence, while width did not.

Downstream of ID 64, active channel width is nearly stable at IDs 68, 69 and 71, while both vegetation width (Fig. S3) and water width (Fig. 9b) show modest increases. Within a fixed active belt this implies that unvegetated bar area is being converted to both water and vegetation. Because bar loss is partitioned between inundation and stabilisation, the reduction in bar area is not by itself diagnostic of sediment starvation, and H_2 is at most weakly supported in this

https://doi.org/10.5194/egusphere-2026-6100
Preprint. Discussion started: 11 November 2026
© Author(s) 2026. CC BY 4.0 License.

reach. Any sediment deficit present is more plausibly sourced from extraction upstream of Delhi (H_3) than from reservoir trapping.

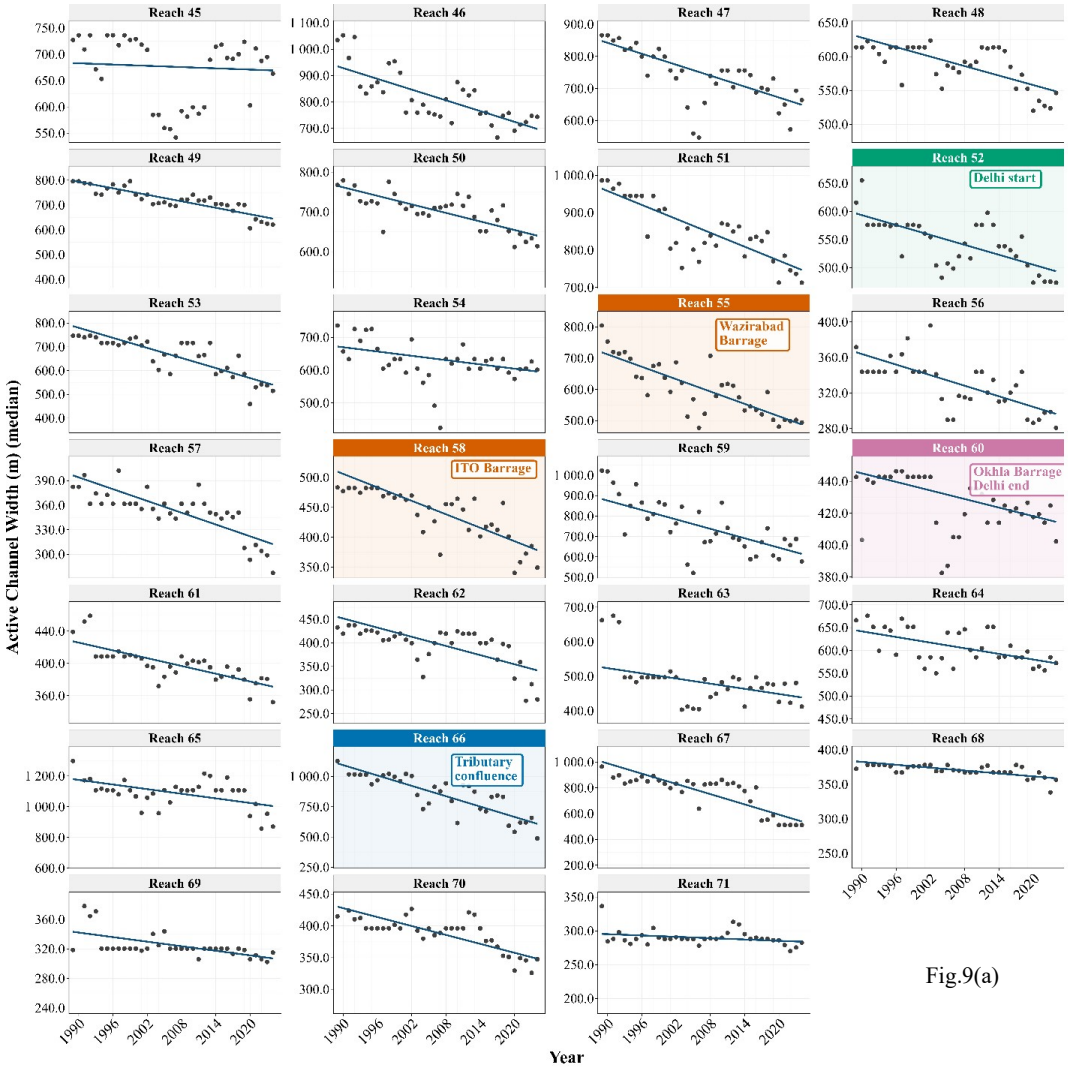


Fig.9(a)

https://doi.org/10.5194/egusphere-2026-6100
Preprint. Discussion started: 11 November 2026
© Author(s) 2026. CC BY 4.0 License.

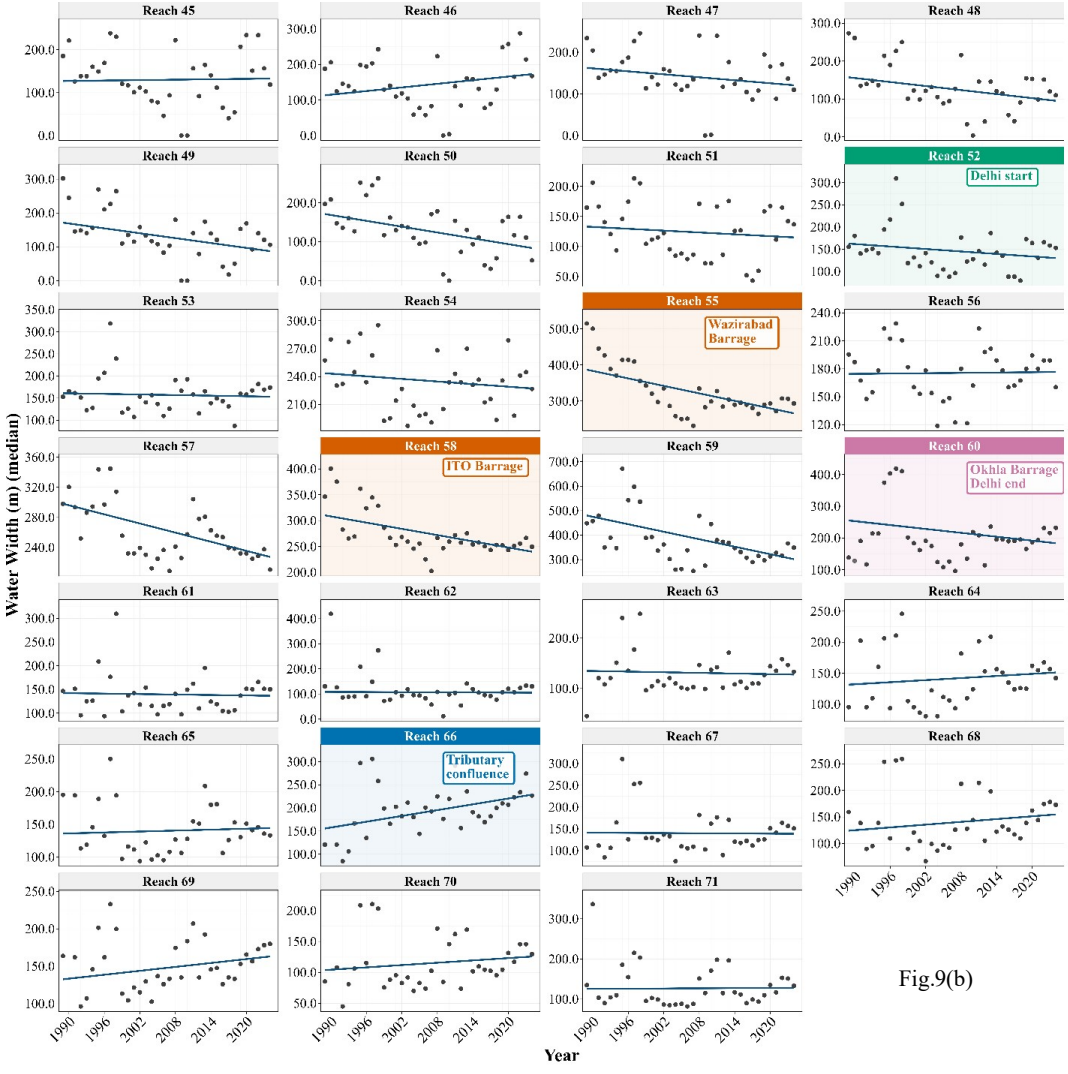


Fig.9(b)

Figure .9(a) Variation of yearly median active channel width and 8(b)Variation of yearly median Water width from Reach ID = 45 to Reach ID=71 along the segment 3 from Reach ID = 45 to Reach ID=71

5.3.4 Segment-4: Reach further downstream of Delhi (> IDs 72)

This segment initiates 60 km downstream of the Delhi megacity (IDs 72 to 92). This downstream segment is characterized by a laterally unconfined single-channel Geomorphic Setting. Active channel width (ACW) shows predominantly negative slopes, following two patterns: a gradual decline through time in some reaches, and abrupt local shifts in others. Neither pattern propagates systematically in the downstream direction. This absence of downstream propagation argues against a dam-driven sediment-starvation signal (H_2), which would be expected to attenuate progressively downstream of the impoundment (Fig. 4f). The scattered, abrupt reductions instead point to

https://doi.org/10.5194/egusphere-2026-6100
Preprint. Discussion started: 11 November 2026
© Author(s) 2026. CC BY 4.0 License.

distributed sediment mining within and upstream of the city as the driving control, consistent with hypothesis H_3 which suggests an uniform mining across the segment and a uniform channel narrowing after that. Vegetation width (VGW) shows a consistent increasing trend with low to moderate positive slopes (Supplementary Material, Fig. S4). The rate of increase remains relatively uniform across the reach, similarly to the water width that increases as well.

Water width (WW) displays a gentle increasing trend along most IDs within this segment (Fig. 10b), although the higher-flow period before 1999 is still discernible. Following the tributary confluence, WW values remain relatively stable, with only minor interannual variability. The braiding index (BI) shows a similar increasing tendency, with gradual positive slopes across the reach (Fig. S8, Supplement). This reach resembles the one observed between ID 64 and ID 71, but occurs in a context of active channel width decline. Bar disappearance in these single-thread reaches responds somewhat differently than in the braided reach upstream part of study area: here, bars are replaced partly by vegetation and partly by water, driven by upstream and local mining activity.

https://doi.org/10.5194/egusphere-2026-6100
Preprint. Discussion started: 11 November 2026
© Author(s) 2026. CC BY 4.0 License.

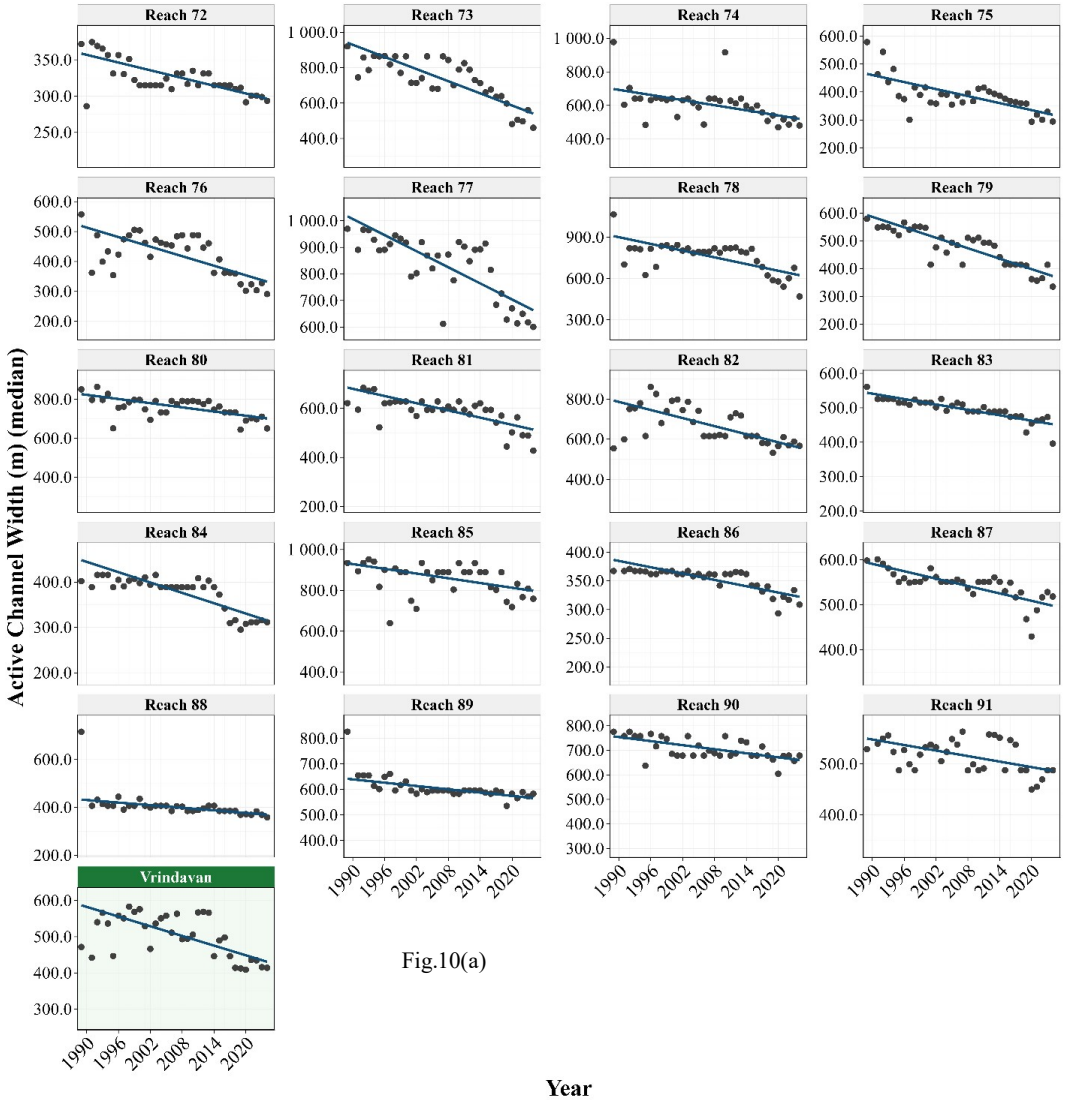


Fig.10(a)

517

https://doi.org/10.5194/egusphere-2026-6100
Preprint. Discussion started: 11 November 2026
© Author(s) 2026. CC BY 4.0 License.

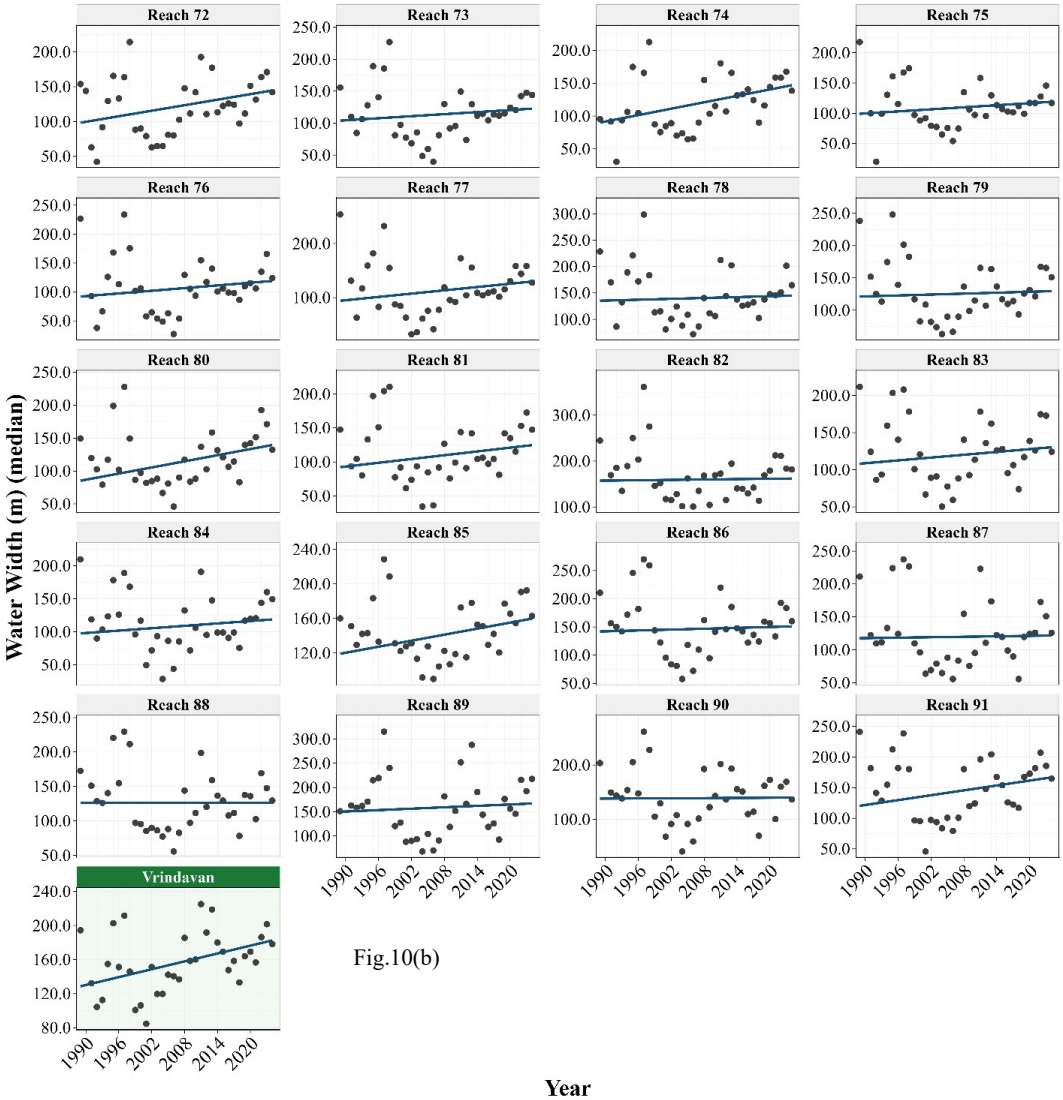


Fig.10(b)

Figure.10(a) Variation of yearly median active channel width and 9(b) Variation of yearly median water width along the segment 4 from Reach ID = 72 to Reach ID=92 (Vrindavan)

6. Discussion

6.1 Identification and Differentiation of anthropogenic pressures

The geomorphic behavior related to riverscape changes of the Yamuna River along the study reach reflects the compound influence of multiple anthropogenic pressures operating across different spatial and temporal scales. A central challenge in interpreting the observed channel changes with specific drivers is equifinality (Chorley, 1962).

https://doi.org/10.5194/egusphere-2026-6100
Preprint. Discussion started: 11 November 2026
© Author(s) 2026. CC BY 4.0 License.

Understanding the cause-effect relationship linked with specific drivers is needed to identify adapted solutions for river rejuvenation. In this case, the flow regulation through dam, sediment extraction and megacity pressure each produce morphologically similar outcomes, making it difficult to isolate dominant controls from present day records alone. The temporal structure of the observed changes, however, provides a basis for differentiation. The absence of a distinct chronological break in active channel width (ACW) immediately following the dam activity (2002), combined with the most pronounced structural break occurring in 2011–2012 in spatial coincidence with intensified gravel extraction at reaches ID 10–14, argues against flow regulation as the primary driver of the geomorphic change or sediment starvation due to reservoir sediment trapping. Instead it indicates sediment extraction as the dominant geomorphic control. Further, we do not see any effect of Hd on the peak flow series (Fig.S10). We also observed a similar narrow channel upstream and downstream of the Hathinikund Dam (Fig. S12, Supp. Mat.), a few years before the dam operated. In general, dams cause an asymmetric response in channel width; wider upstream due to the reservoir and narrower downstream due to sediment trapping and restricted water release (Brandt,2000; Graf, 2006; Khaleghi et al.,2025). Hence, the impact of the reservoir on water width is not apparent in the reaches, because of the smaller size (<1 km) of Hathinikund reservoir. In the absence of a direct impact of the Hd on sediment transport and peak flows, the role of sediment mining is important in the 75 km Yamuna river from dam to Delhi NCR region. This channel length is characterised by unique geomorphic and riverscape signatures, which can only be explained by gravel/sand mining activities. It includes strong oscillatory behaviour in ACW rather than unidirectional narrowing, disproportional relationship between discharge and water width and morphological change from braided to meandering river. Oscillatory behaviour in ACW reflects a disturbed sediment budget in which episodic extraction is only partially offset by monsoon-season replenishment. The incomplete recovery between extraction cycles produces a progressive adjustment toward a narrower, more constrained geometry. The spatial coherence of this narrowing signal across multiple reaches confirms that mining operation at a reach to segment-scale acts as a driver for overwhelming local hydrological variability. This signal intensified markedly after 2011, is consistent with satellitedocumented extraction activity (Yadav et al., 2023).

The discharge and water width relationship provides a further diagnostic. Ten-daily discharge records at ID=5, 17, 37, 57, and even 71 show only minor reductions in mean discharge (Fig. 3), yet these are accompanied by disproportionately large declines in water width, a departure from expected hydraulic geometry scaling (Fig.6) (Leopold and Maddock, 1953; Wohl and Merritt, 2008). This decoupling suggests that the channel has undergone fundamental cross-sectional reorganization through incision driven by sediment extraction and starvation all along the reach, such that width no longer adjusts freely to discharge variability. It is similar with field observations in Italian rivers, where gravel extraction triggered persistent incision, bed coarsening, and planform simplification lasting decades after mining ceased (Surian and Rinaldi, 2003; Rinaldi et al., 2005).

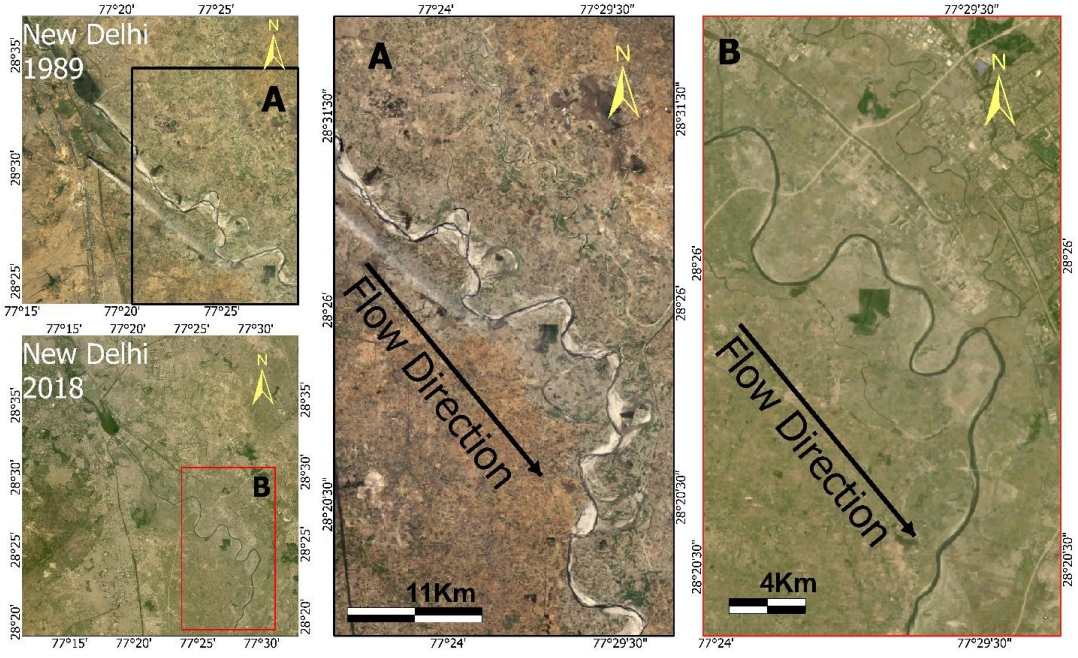
The concurrent transition from a braided planform to a predominantly single-thread morphology reinforces this interpretation and has significant implications for recovery potential. Braided rivers maintain geomorphic dynamism through bar reworking, lateral migration, and channel switching while single-thread incised systems lack this selforganizing capacity (Brierley and Fryirs, 2005; Church,2006). The crossing of this planform threshold, therefore, represents not merely a descriptive shift in channel style but a reduction in intrinsic geomorphic resilience. Recovery

https://doi.org/10.5194/egusphere-2026-6100
Preprint. Discussion started: 11 November 2026
© Author(s) 2026. CC BY 4.0 License.

to a braided state would require not only the cessation of extraction but also the reintroduction of sufficient sediment flux to rebuild bars and re-establish characteristic width-to-depth ratios, a process that may take decades even under favorable conditions (Fryirs and Brierley, 2016; Wohl et al., 2015). In a sense, the large braided pattern of the Yamuna in the current context has definitely disappeared (Fig.S11).

Delhi urbanization and further mining activity in the downstream urban section of the Yamuna induce a typical progressive erosion further downstream, in a context where local mining also occurs. Though the river is gaining water through base flow and tributary contribution downstream of Delhi, it is still not able to regain its morphological characteristics. This adjustment in a single-bed channel induced different planform modifications compared to the upstream braided section, with a slight water channel widening and a partial vegetation encroachment. This impact is visible in Fig.11, where the dynamic channel of 1989 with its meander scars is now disconnected from the floodplains in 2018. Despite the negligible difference in water width of both these years, the river space has shrunk with very little sediment. This is also validated by field observations (Fig. 12). The observed multi-thread-to-single-thread adjustment may be due to bed incision caused by sediment starvation, analogous to clear-water release effects documented downstream of large dams (Williams and Wolman, 1984; Kondolf, 1997). The concurrent progressive increase in vegetation width corroborates geomorphic stabilization. Riparian vegetation encroachment is a well-documented response to reduced flow energy and sediment supply (Bertoldi et al., 2011; Gurnell, 2014), and once established, it exerts a positive feedback by increasing bank cohesion, trapping fine sediment, and raising the threshold discharge required for bank erosion, effectively locking in the narrowed single channel morphology and further reducing recovery capacity. The Yamuna River segment downstream of Delhi is characterized by insignificant sediment transport and is geomorphologically inactive (Bawa et al.,2014). A new equilibrium of a single-channel meandering river has been set up for the originally braided Himalayan river.

https://doi.org/10.5194/egusphere-2026-6100
Preprint. Discussion started: 11 November 2026
© Author(s) 2026. CC BY 4.0 License.



583

584 **Figure 11. Channel change downstream of Delhi between 1989 and 2018. (A) In 1989, the Yamuna had a wide, dynamic**
585 **channel with meander scars; (B) by 2018, the channel had narrowed, incised, and become disconnected from its floodplain.**
586 **True-colour composites produced in Google Earth Engine from Landsat 5 (1989) and Landsat 8 (2018) imagery; Landsat**
587 **imagery courtesy of the U.S. Geological Survey.**



588

589 **Figure 12: Field observations in the downstream of Delhi, showing disconnectivity of the channel from the floodplain.**

https://doi.org/10.5194/egusphere-2026-6100
Preprint. Discussion started: 11 November 2026
© Author(s) 2026. CC BY 4.0 License.

Overall, the geomorphic evolution of the Yamuna River is best understood not through universal models but through the place-based, temporally grounded framework advocated by Brierley and Fryirs (2013). Complexity, contingency, and emergence are central to interpreting the character, behaviour, and evolution of any given river system (Brierley and Fryirs, 2013). The river's non-linear, stage-wise adjustments, where different drivers dominate at different times and locations, confirm that riverscape configuration and channel morphology is the product of interacting controls whose relative influence varies across the landscape and through time, and whose interpretation demands the deep, place-rooted knowledge and carefully related to pressure and response chronology to detect co-occurrence and propagation change, that only a combined reading of the riverscape signature and physical record and long-term satellite archive can provide.

6.2 Time series remote sensing data for process-understanding of riverscape and geomorphic systems

Geomorphic processes operate over spatio-temporal scales that are rarely captured by field observations or short-term monitoring, making long-term, spatially continuous datasets essential for understanding river adjustment. The 35-year Landsat–Sentinel time series (1989–2024), processed on a GEE-based web platform- using MNDWI, NDWI, and NDVI satellite images-derived thresholding, provides such a record for the Yamuna River, enabling the isolation of riverscape responses to dam regulation, sediment mining, and megacity pressure as sequential stages of system-wide change. Large-scale cloud-based platforms now allow fluvial analyses to be extended to petabyte-scale datasets, with threshold-based classification of riverscape features, such as wetted channels, bare sediment, and vegetated surfaces, using multiple spectral indices within a single framework (Boothroyd et al., 2021). This multi-index approach is particularly important in the Yamuna River, where distinguishing vegetated bar encroachment from exposed sediment requires independent use of NDVI.

The annual temporal resolution of this dataset of the Yamuna River enables the detection of both gradual and abrupt riverscape responses. Schwenk et al. (2017) show that yearly Landsat-derived channel masks can resolve multi-scale variability in channel migration, erosion–accretion patterns, and width adjustments, allowing separation of local and climatic influences. Applied here, this resolution supports a before–and–after control–impact framework that distinguishes abrupt WW narrowing linked to changes in flow channel geometry and complex ACW narrowing longitudinal patterns, both associated with active mining activities. Importantly, geomorphic responses to anthropogenic disturbance are often non-linear, governed by the timing, intensity, and duration of external pressures (Verstraeten et al., 2018). The multi-decadal archive, therefore, provides the temporal depth required to identify threshold-driven transitions alongside cumulative adjustments, offering a robust basis for interpreting long-term channel evolution under interacting human stressors. Thus, integrating temporal and spatial variation across different reaches provides a framework to separate the signals of competing drivers for each segment.

7. Conclusions

Major conclusions from the study on anthropogenic impact on a major Himalayan river are as follows:

https://doi.org/10.5194/egusphere-2026-6100
Preprint. Discussion started: 11 November 2026
© Author(s) 2026. CC BY 4.0 License.

1. The Yamuna River, being fairly large, spanning diverse geomorphic settings from confined Himalayan foothills to alluvial plains, and undergoing some fairly recent human pressures that may impact the channel planform, makes it an ideal system for long-term Landsat-based monitoring, providing the channel width and longitudinal continuity necessary for meaningful planimetric analysis.

2. All along the reach, sediment mining has emerged as the dominant contemporary driver of riverscape and geomorphic change, surpassing dam-induced flow regulation in its immediacy and spatial intensity as well as potential water diversion. Rapid urban expansion in Delhi from the early 2000s drove intensified gravel and sand extraction, disrupting the river's sediment budget and forcing measurable channel adjustment. This is expressed as non-linear impacts as widespread narrowing of the active and flow channels (as shown by the shift in WW-Q relationships) but sometimes river is widening (where mining is very ongoing and channel is unadjusted yet). This has led to riverscape and morphological simplification, constituting a direct and measurable perturbation to the process–form relationships that had previously adjusted, however partially, to regulated flow conditions.

3. Hypothesis-driven BACI analysis based on multi-decadal remote sensing time series, processed through a combined MNDWI, NDWI, and NDVI thresholding framework on a GEE-based web application, proved an effective and irreplaceable approach for establishing cause–impact relationships across a river system subjected to multiple, temporally staggered anthropogenic stressors. By preserving the chronological order of disturbance, barrage regulation, and sediment mining, the dataset enabled the sequential attribution of riverscape change to specific drivers, a resolution that neither field campaigns nor short-record monitoring could have achieved.

Supplement Link

Link to the supplementary file-
https://docs.google.com/document/d/1h4b5mHAz32TwNzXLyJ2ppldXOYiPEre6B8Kn7Wh48c/edit?tab=t.0

Author's Contribution

SS performed data curation, formal analysis, investigation, and methodology, produced the visualizations, and prepared the original draft. RL contributed to data curation, methodology, and software. NK contributed to initial data curation. BB contributed to conceptualization, methodology, and visualization, and reviewed and edited the manuscript. HP contributed to conceptualization, funding acquisition, project administration, and supervision, and reviewed and edited the manuscript. VJ contributed to conceptualization, project administration, and supervision, and reviewed and edited the manuscript. All authors read and approved the final manuscript.

Competing interests

The authors declare no conflicts of interest.

Acknowledgments

https://doi.org/10.5194/egusphere-2026-6100
Preprint. Discussion started: 11 November 2026
© Author(s) 2026. CC BY 4.0 License.

This work was supported by the French National Research Agency (ANR), in the frame of the project 'GloUrb' (ANR-22-CE03-0005), co-funded by 'LABoratoire d'EXcellence Intelligences desMondes Urbains' (ANR-10-LABX-0088) and the 'Ecole Universitaire de Recherche H2O'Lyon' (ANR-17-EURE-0018) within the programme 'Investissements d'Avenir' operated by ANR.B. Belletti's contribution is framed within the CPJ 'Hydrosystèmes' supported by the French National Research Agency (ANR-23-CPJ1-0148-01).

8. References

Arnaud, F., Piégay, H., Schmitt, L., Rollet, A., Ferrier, V., and Béal, D. :Historical geomorphic analysis (1932–2011) of a by-passed river reach in process-based restoration perspectives: The Old Rhine downstream of the Kembs diversion dam (France, Germany), Geomorphology, 236, 163-177, 10.1016/j.geomorph.2015.02.009, 2015.

Balha, A., Vishwakarma, B. D., Pandey, S., and Singh, C. K.: Predicting impact of urbanization on water resources in megacity Delhi, Remote Sensing Applications: Society and Environment, 20, 100361, https://doi.org/10.1016/j.rsase.2020.100361,2020.

Bawa, N., Jain, V., Shekhar, S., Kumar, N., and Jyani, V.: Controls on morphological variability and role of stream power distribution pattern, Yamuna River, western India. Geomorphology, 227, 60-72, https://doi.org/10.1016/j.geomorph.2014.05.016, 2014.

Bertoldi, W., Drake, N.A. and Gurnell, A.M.: Interactions between river flows and colonizing vegetation on a braided river: exploring spatial and temporal dynamics in riparian vegetation cover using satellite data, Earth Surface Processes and Landforms, 36, 1474-1486, https://doi.org/10.1002/esp.2166 , 2011.

Bertrand, M., and Liébault, F.: Active channel width as a proxy of sediment supply from mining sites in New Caledonia, Earth Surface Processes and Landforms, 44, 67-76, 10.1002/esp.4478, 2018.

Best, J.: Anthropogenic stresses on the world's big rivers, Nature Geoscience, 12, 7–21 , https://doi.org/10.1038/s41561-018-0262-x, 2019.

Best, J., and Darby, S. E.: The Pace of Human-Induced Change in Large Rivers: Stresses, Resilience, and Vulnerability to Extreme Events, One Earth, 2, 510-514, https://doi.org/10.1016/j.oneear.2020.05.021, 2020.

Bollati, I. M., Pellegrini, L., Rinaldi, M., Duci, G., and Pelfini, M.: Reach-scale morphological adjustments and stages of channel evolution: The case of the Trebbia River (northern Italy), Geomorphology, 221, 176–186. 10.1016/j.geomorph.2014.06.007, 2014.

https://doi.org/10.5194/egusphere-2026-6100
Preprint. Discussion started: 11 November 2026
© Author(s) 2026. CC BY 4.0 License.

695 Bookhagen, B., and Burbank, D. W.: Toward a complete Himalayan hydrological budget: Spatiotemporal distribution
696 of snowmelt and rainfall and their impact on river discharge, J. Geophys. Res.-Earth, 115(F3),
697 https://doi.org/10.1029/2009JF001426,2010.
698
699 Boothroyd, R.J., Williams, R.D., Hoey, T.B., Barrett, B., Prasojo, O.A.: Applications of Google Earth Engine in fluvial
700 geomorphology for detecting river channel change, WIREs Water,8, https://doi.org/10.1002/wat2.1496, 2021.
701
702 Brandt, S.A.: Classification of geomorphological effects downstream of dams, CATENA, 40, 375-401,
703 https://doi.org/10.1016/S0341-8162(00)00093-X, 2000.
704 Brierley, G., and Fryirs, K. River Styles, a Geomorphic Approach to Catchment Characterization: Implications for River
705 Rehabilitation in Bega Catchment, New South Wales, Australia. Environmental Management, 25, 661–679 ,
706 https://doi.org/10.1007/s002670010052,2000.
707
708 Brierley, G. J. and Fryirs, K. A.: Geomorphology and river management: applications of the River Styles Framework,
709 Blackwell Publishing, Oxford, 398 pp, ISBN 9780632064894, https://doi.org/10.1002/9780470751367, 2005.
710
711 Brierley, G.J., Fryirs, K.A., Cullum, C., Tadaki, M., Huang, H.Q., and Blue, B.: Reading the landscape: Integrating
712 the theory and practice of geomorphology to develop place-based understandings of river systems. Progress in Physical
713 Geography , 37(5), 601–621, https://doi.org/10.1177/0309133313490007, 2013.
714
715 Chatterjee, R., Gupta, B.K., Mohiddin, S.K., Singh, P.N., and Shekhar, S.: Dynamic groundwater resources of
716 National Capital Territory, Delhi: assessment, development and management options, Environ. Earth Sci., 59, 669–
717 686, https://doi.org/10.1007/s12665-009-0064-y, 2009.
718
719 Chin, A.: Urban transformation of river landscapes in a global context, Geomorphology, 79, 460-487,
720 https://doi.org/10.1016/j.geomorph.2006.06.033, 2006.
721
722 Chorley, R. J.: Geomorphology and General Systems Theory, United States: U.S. Government Printing Office,
723 https://doi.org/10.3133/pp500B ,1962.
724
725 Church, M.: Geomorphic response to river flow regulation: Case studies and time-scales, Regul. Rivers: Res. Mgmt.,
726 11, 3-22, https://doi.org/10.1002/rrr.3450110103,1995.
727
728 Church, M.: Bed material transport and the morphology of alluvial river channels, Annu. Rev. Earth Pl. Sc., 34, 325–
729 354, https://doi.org/10.1146/annurev.earth.33.092203.122721, 2006.
730
731 Clerici, A., Perego, S., Chelli, A. and Tellini, C.: Morphological changes of the floodplain reach of the Taro River

https://doi.org/10.5194/egusphere-2026-6100
Preprint. Discussion started: 11 November 2026
© Author(s) 2026. CC BY 4.0 License.

(Northern Italy) in the last two centuries, Journal of Hydrology, 527, 1106-1122, 10.1016/j.jhydrol.2015.05.063,2015.

Collins, B., and Dunne, T.: Fluvial Geomorphology and River-Gravel Mining: A Guide for Planners, case studies included, Special Publication 98, California Department of Conservation, Division of Mines and Geology, https://archive.org/details/fluvialgeomorpho98coll,1990.

Costigan, K. H., and Daniels, M. D.: Damming the prairie: Human alteration of Great Plains river regimes, Journal of Hydrology, 444, 90-99, https://doi.org/10.1016/j.jhydrol.2012.04.008,2012.

Damseth S., Thakur, K., Kumar R., Kumar S., Mahajan D., Kumari H., Sharma D., and Sharma A. K.: Assessing the impacts of river bed mining on aquatic ecosystems: A critical review of effects on water quality and biodiversity, HydroResearch, 7, 122–130, https://doi.org/10.1016/j.hydres.2024.01.004, 2024.

Downs, P. W. and Piégay, H.: Catchment-scale cumulative impact of human activities on river channels in the late Anthropocene: implications, limitations, prospect, Geomorphology, 338, 88–104, https://doi.org/10.1016/j.geomorph.2019.03.021, 2019.

Downs, P. and Gregory, K. (1st Edition): River channel management: towards sustainable catchment hydrosystems, Routledge, London, 408pp, ISBN 9780203770344, https://doi.org/10.4324/9780203770344, 2014.

Dudgeon, D., Arthington, A.H., Gessner, M.O., Kawabata, Z. I., Knowler, D.J., Lévêque, C., Naiman, R.J., PrieurRichard, A. H., Soto, D., Stiassny, M.L.J. and Sullivan, C.A.: Freshwater biodiversity: importance, threats, status and conservation challenges, Biological Reviews, 81, 163-182, https://doi.org/10.1017/S1464793105006950, 2006.

Dudgeon, D.: Multiple threats imperil freshwater biodiversity in the Anthropocene, Current Biology, 29, R960–R967, https://doi.org/10.1016/j.cub.2019.08.002, 2019.

Dufour, S., Rinaldi, M., Piégay, H., and Michalon, A.: How do river dynamics and human influences affect the landscape pattern of fluvial corridors? Lessons from the Magra River, Central–Northern Italy, Landscape and Urban Planning, 134, 107-118, https://doi.org/10.1016/j.landurbplan.2014.10.007, 2015.

Dunesme, S., Belletti, B., Helling, L., and Limonet, J.: EVS-GIS/glourbee, UMR5600 Environnement, Ville, Société. https://doi.org/10.5281/zenodo.11235572 ,2024.

Ekka, A., Pande, S., Jiang, Y. and van der Zaag, P.: Anthropogenic Modifications and River Ecosystem Services: A Landscape Perspective, Water, 12, 10.3390/w12102706, 2020.

https://doi.org/10.5194/egusphere-2026-6100
Preprint. Discussion started: 11 November 2026
© Author(s) 2026. CC BY 4.0 License.

766 Feyisa, G. L., Meilby, H., Fensholt, R., and Proud, S. R.:Automated Water Extraction Index: A new technique for
767 surface water mapping using Landsat imagery, Remote sensing of environment,140, 23-35,
768 https://doi.org/10.1016/j.rse.2013.08.029, 2014.
769
770 Friedman, Osterkamp, W.R., Scott, M.L. and Auble, G.T.: Downstream effects of dams on channel geometry and
771 bottomland vegetation: Regional patterns in the great plains, Wetlands, 18, 619–633,
772 https://doi.org/10.1007/BF03161677,1998.
773
774 Friedman, J. M., Eurich, A. M., Auble, G. T., Scott, M. L., Shafroth, P. B., and Gibson, P. P.: Response of riparian
775 vegetation to short-and long-term hydrologic variation, Ecological Applications, 32(8),
776 https://doi.org/10.1002/eap.2689,2022.
777
778 Fryirs, K.A. and Brierley, G.J. :Assessing the geomorphic recovery potential of rivers: forecasting future trajectories
779 of adjustment for use in management, WIREs Water, 3, 727-748, https://doi.org/10.1002/wat2.1158,2016.
780
781 Fryirs, K. A., Brierley, G. J., Preston, N. J., and Kasai, M.: Buffers, barriers and blankets: The (dis)connectivity of
782 catchment-scale sediment cascades, CATENA,70,49-67, https://doi.org/10.1016/j.catena.2006.07.007,2007.
783
784 Galay,V.J.: Causes of river bed degradation, Water resources research, 19(5), 1057-
785 1090, https://doi.org/10.1029/WR019i005p01057,1983.
786
787 Geerling, G. W., Ragas, A. M. J., Leuven, R. S. E. W., Van den Berg, J. H., Breedveld, M., Liefhebber, D., and Smits,
788 A. J. M.:Succession and rejuvenation in floodplains along the river Allier (France), Hydrobiologia, 565(1), 71-86,
789 https://doi.org/10.1007/s10750-005-1906-6,2006.
790
791 Giller, P. S.: River restoration: seeking ecological standards, Journal of applied ecology, 42(2), 201–207,
792 https://doi.org/10.1111/j.1365-2664.2005.01020.x,2005.
793
794 Graf, W. L.: Downstream hydrologic and geomorphic effects of large dams on American rivers, Geomorphology, 79,
795 336-360, https://doi.org/10.1016/j.geomorph.2006.06.022,2006.
796
797 Gupta, A.: Urban hydrology and sedimentation in the humid tropics, in: Developments and Applications of
798 Geomorphology, edited by: Costa, J. E. and Fleisher, P. J., Springer, Berlin, Heidelberg, https://doi.org/10.1007/9783-
799 642-69759-3_8, 1984.
800
801 Gurnell, A.: Plants as river system engineers, Earth Surface Processes and Landforms, 39, 4-25.
802 https://doi.org/10.1002/esp.3397,2014.

https://doi.org/10.5194/egusphere-2026-6100
Preprint. Discussion started: 11 November 2026
© Author(s) 2026. CC BY 4.0 License.

Hackney, C. R., Vasilopoulos, G., Heng, S., Darbari, V., Walker, S., and Parsons, D. R.: Sand mining far outpaces natural supply in a large alluvial river, Earth Surface Dynamics, 9(5), 1323-1334,https://doi.org/10.5194/esurf-91323-2021, 2021.

Henshaw, A. J., Gurnell, A. M., Bertoldi, W., and Drake N. A.: An assessment of the degree to which Landsat TM data can support the assessment of fluvial dynamics, as revealed by changes in vegetation extent and channel position, along a large river, Geomorphology, 202, 74-85, https://doi.org/10.1016/j.geomorph.2013.01.011,2013.

Hong, L.B., and Davies, T.: A study of stream braiding, Geological Society of America Bulletin*, 90*, 1839-1859, https://api.semanticscholar.org/CorpusID:129279187, 1979.

Jha, P.K., Subramanian, V., and Sitasawad, R.: Chemical and sediment mass transfer in the Yamuna River - A tributary of the Ganges system, Journal of Hydrology, 104, 237-246, https://doi.org/10.1016/0022-1694(88)90167-9, 1988.

Jha, P., Kumar, P. Y., Joy, M. S., Bansal, T., and Jha, A. N.: Crossing the ecological threshold: Spatio-temporal dynamics of blue-green space ecosystem health in Delhi using a VORR framework, Environmental and Sustainability Indicators, 30, https://doi.org/10.1016/j.indic.2026.101243,2026.

Joshi, P., Chauhan, A., Dua, P.,Malik,S.,and Liou,Y-A.: Physicochemical and biological analysis of river Yamuna at Palla station from 2009 to 2019, Scientific Reports 12, 2870, https://doi.org/10.1038/s41598-022-06900-6,2022.

Kempton, R. A., and Green, R. H.: Sampling Design and Statistical Methods for Environmental Biologists, Biometrics, 37(1), 202, https://doi.org/10.2307/2530544,1981.

Khaleghi, S., and Nosrati, K.:Uneven understanding of morphological impacts of dams: upstream vs. downstream. Frontiers in Environmental Science, 13, 162616510.3389/fenvs.2025.1626165, 2025.

Koehnken, L., Rintoul, M.S., Goichot, M., Tickner, D., Loftus. A-C., and Acreman M.C.: Impacts of riverine sand mining on freshwater ecosystems: A review of the scientific evidence and guidance for future research, River Research and Applications, 36, 362–370, https://doi.org/10.1002/rra.3586,2020.

Kondolf, G.M.: Hungry Water: Effects of Dams and Gravel Mining on River Channels, Environmental Management, 21, 533 –551, https://doi.org/10.1007/s002679900048, 1997.

Kondolf, G. M.: Geomorphic and environmental effects of instream gravel mining, Landscape and Urban Planning, 28, 225-243, https://doi.org/10.1016/0169-2046(94)90010-8, 1994.

https://doi.org/10.5194/egusphere-2026-6100
Preprint. Discussion started: 11 November 2026
© Author(s) 2026. CC BY 4.0 License.

Kumar, M., Sharif, M., and Ahmed, S. : Flood estimation at Hathnikund Barrage, River Yamuna, India using the Peak-Over-Threshold method, ISH Journal of Hydraulic Engineering, *26*(3), 291–300, https://doi.org/10.1080/09715010.2018.1485119, 2018.

Lallias-Tacon, S., Liébault, F., and Piégay, H.: Use of airborne LiDAR and historical aerial photos for characterising the history of braided river floodplain morphology and vegetation responses, Catena, 149, 742-759. https://doi.org/10.1016/j.catena.2016.07.038, 2017.

Lemm, J.U., Venohr, M., Globevnik, L., Stefanidis, K., Panagopoulos, Y., van Gils, J., Posthuma, L., Kristensen, P., Feld, C.K., Mahnkopf, J., Hering, D. and Birk, S.: Multiple stressors determine river ecological status at the European scale: Towards an integrated understanding of river status deterioration. Global Change Biology, 27, 1962-1975. https://doi.org/10.1111/gcb.15504, 2021.

Leopold, L. B. and Maddock, T.: The hydraulic geometry of stream channels and some physiographic implications, U.S. Geological Survey Professional Paper 252, U.S. Government Printing Office, Washington, D.C., 57 pp., https://doi.org/10.3133/pp252, 1953.

Lima, A. C., Sayanda, D., and Wrona, F. J.: A roadmap for multiple stressors assessment and management in freshwater ecosystems, Environmental Impact Assessment Review, 102, 107191, https://doi.org/10.1016/j.eiar.2023.107191, 2023.

McFEETERS, S. K.: The use of the Normalized Difference Water Index (NDWI) in the delineation of open water features, International Journal of Remote Sensing, 17(7), 1425–1432, https://doi.org/10.1080/01431169608948714, 1996.

Meybeck, M.: Global analysis of river systems: From Earth system controls to Anthropocene syndromes, Philosophical transactions of the Royal Society of London, Biological sciences, 358, 1935-55. 10.1098/rstb.2003.1379, 2003.

Mittal, R., Said, S., and Beg, M.: Assessment of Changes in Planform Morphology of the Upper Yamuna River Segment, India, Using Remote Sensing and GIS, Physical Geography, 44(4), 446–477. https://doi.org/10.1080/02723646.2022.2090656,2023.

Mohanty, M. and Tare, V.: Quantifying anthropogenic interventions in Yamuna River through river flow health index and geomorphic analysis, Research Square [preprint], https://doi.org/10.21203/rs.3.rs-2836493/v1, 2023.

Morel, M., Tamisier, V., Pella, H., Booker, D. J., Navratil, O., Piégay, H., Gob, F., and Lamouroux, N.: Revisiting the drivers of at-a-station hydraulic geometry in stream reaches, Geomorphology, 328, 44-56, https://doi.org/10.1016/j.geomorph.2018.12.007, 2019.

https://doi.org/10.5194/egusphere-2026-6100
Preprint. Discussion started: 11 November 2026
© Author(s) 2026. CC BY 4.0 License.

Ollero, A.: Channel changes and floodplain management in the meandering middle Ebro River, Spain. Geomorphology, 117,247-260, 10.1016/j.geomorph.2009.01.015,2010.

Orr, J. A., Vinebrooke, R. D., Jackson, M. C., Kroeker, K. J., Kordas, R. L., Mantyka-Pringle, C., Van den Brink, P.J., De Laender, F., Stoks, R., Holmstrup, M., Matthaei, C.D., Monk, W.A., Penk, M.R., Leuzinger, S., Schäfer, R.B., Piggott, J.J.: Towards a unified study of multiple stressors: divisions and common goals across research disciplines. Proceedings of the Royal Society B: Biological Sciences, 287, https://doi.org/10.1098/rspb.2020.0421,2020.

Patel, N. K., Schlunegger, F., Mair, D., Pati, P., Prado, A. H., Garefalakis, P., and Choudhury, R. K., Source-to-sink patterns of grain size along the Yamuna River in the Indian Himalaya, Geomorphology, 486, https://doi.org/10.1016/j.geomorph.2025.109909,2025.

Peipoch, M., Brauns, M., Hauer, F. R., Weitere, M., and Valett, H. M.: Ecological Simplification: Human Influences on Riverscape Complexity, BioScience, 65, 1057–1065, https://doi.org/10.1093/biosci/biv120, 2015.

Pekel, JF., Cottam, A., Gorelick, N., and Belward, A.S.: High-resolution mapping of global surface water and its longterm changes, Nature, 540, 418–422 , https://doi.org/10.1038/nature20584,2016.

Quick, L., Williams, R.D., Boothroyd, R.J., Hoey, T.B., Tolentino, P.L.M., MacDonell, C., Guardian,E, Reyes,J., Sabillo, C., Perez, J., and David, C.P.C.: Confined and mined: anthropogenic river modification as a driver of flood risk change, npj Nat. Hazards 2, 4 , https://doi.org/10.1038/s44304-024-00051-6,2025.

Rai, R. K., Upadhyay, A., Ojha, C. S. P., and Singh, V. P.: Water resources and water budgeting, in: The Yamuna River Basin: Water Resources and Environment, Water Science and Technology Library, vol. 66, Springer, Dordrecht, https://doi.org/10.1007/978-94-007-2001-5_8, 2012.

Rentier ,E.S., and Cammeraat, L.H.: The environmental impacts of river sand mining, Science of The Total Environment, 838, https://doi.org/10.1016/j.scitotenv.2022.155877,2022.

Rinaldi, M., Wyżga, B., and Surian, N.: Sediment mining in alluvial channels: physical effects and management perspectives, River Research and Application, 21,805-828, https://doi.org/10.1002/rra.884,2005.

Rollet, A. J., Piégay, H., Dufour, S., Bornette, G., and Persat, H.: Assesment of Consequences of Sediment Deficit on a Gravel River Bed Downstream of Dams in Restoration Perspectives: Application of a Multicriteria, Hierarchical and Spatially Explicit Diagnosis, River Research and Application, 30, 939–953,10.1002/rra.2689, 2014.

Roux C., Alber A., Bertrand M., Vaudor, L., and Piégay, H.: “FluvialCorridor”: A New ArcGIS Toolbox Package for

https://doi.org/10.5194/egusphere-2026-6100
Preprint. Discussion started: 11 November 2026
© Author(s) 2026. CC BY 4.0 License.



914 Multiscale Riverscape Exploration, Geomorphology, 242, 29–37,
915 https://doi.org/10.1016/j.geomorph.2014.04.018,2015.

916 Schwenk, J., Khandelwal, A., Fratkin, M., Kumar, V., and Georgiou, E.F.: High spatiotemporal resolution of river
917 planform dynamics from Landsat: The RivMAP toolbox and results from the Ucayali River, Earth and Space Science,
918 4, 46–75, 10.1002/2016EA000196,2017.
919
920 Seger, K., Sousa-Lima, R., Schmitter-Soto, J., and Urban, E.: Editorial: Before-After Control-Impact (BACI) studies
921 in the ocean, Frontiers in Marine Science, 8, 787959, https://doi.org/10.3389/fmars.2021.787959, 2021.
922
923 Segura, S.F., and Sanchis-Ibor, C.: Assessment of channel changes in a Mediterranean ephemeral stream since the
924 early twentieth century. The Rambla de Cervera, Eastern Spain, Geomorphology, 201,
925 10.1016/j.geomorph.2013.06.021,2013.
926
927 Segurado, P., Gutierrez-Canovas, T., Ferreira, T., and Branco, P.: Stressor gradient coverage affects interaction
928 identification, Ecological Modeling, 472, https://doi.org/10.1016/j.ecolmodel.2022.110089,2022.
929
930 Sharma, M., and Abhay, R.K.: Urban growth and quality of life: inter-district and intra-district analysis of housing in
931 NCT-Delhi, 2001–2011–2020, GeoJournal ,87, 797–819, https://doi.org/10.1007/s10708-021-10570-8,2022.
932
933 Sharma, M., Rawat, S., Kumar, D., Awasthi, A., Sarkar, A., Sidola, A., Choudhary, T., and Kotecha, K.: The state of
934 the Yamuna River: a detailed review of water quality assessment across the entire course in India, Applied Water
935 Science, 14, 175 , https://doi.org/10.1007/s13201-024-02227-x,2024.
936
937 Sharma, B., Ram, S., and Vyas, S.: Characterization of Yamuna River water quality and its remediation by
938 Phytoremediation technique, South African Journal of Chemical Engineering, 53(1), 49-59,
939 https://hdl.handle.net/10520/ejc-chemeng-v53-n1-a5, 2025.
940 Sinha, R., Akuria, M., Mishra, K. and Sarkar, D.: River Sand Mining: A Developing Geohazard in the Himalaya,
941 10.1007/978-3-031-95083-4_22,2025.
942
943 Surian, N., and Rinaldi, M.: Morphological response to river engineering and management in alluvial channels in Italy,
944 Geomorphology, 50, 307-326, https://doi.org/10.1016/S0169-555X(02)00219-2, 2003.
945
946 Tanya, Tandon, S.K., Gaurav, K. and Singh, V.: Two Centuries of Hydrogeomorphic Changes: Width-Discharge
947 Dynamics of the Urbanised Yamuna River in Delhi, Journal of the Geological Society of India, 102(4),526–536,
948 https://doi.org/10.17491/jgsi/2026/174380, 2026.
949
950 Tickner, D., Opperman, J. J., Abell, R., Acreman, M., Arthington, A. H., Bunn, S. E., Cooke, S. J., Dalton, J., Darwall,

https://doi.org/10.5194/egusphere-2026-6100
Preprint. Discussion started: 11 November 2026
© Author(s) 2026. CC BY 4.0 License.

W., Edwards, G., Harrison, I., Hughes, K., Jones, T., Leclère, D., Lynch, A. J., Leonard, P., McClain, M. E., Muruven, D., Olden, J. D., Ormerod, S. J., Robinson, J., Tharme, R. E., Thieme, M., Tockner, K., Wright, M., and Young, L.: Bending the curve of global freshwater biodiversity loss: an emergency recovery plan, BioScience, 70, 330–342, https://doi.org/10.1093/biosci/biaa002, 2020.

UN DESA (United Nations, Department of Economic and Social Affairs, Population Division): 2018 Revision of World Urbanization Prospects, United Nations, New York, https://desapublications.un.org/publications/2018revision-world-urbanization-prospects (last access: 11 October 2026), 2018.

Verstraeten, G., Notebaert, B., Broothaerts, N., Vandenberghe, J., and De Smedt, P.: River landscapes in the Dijle catchment: from natural to anthropogenic meandering rivers, in: Landscapes and Landforms of Belgium and Luxembourg, edited by: Demoulin, A., World Geomorphological Landscapes, Springer, Cham, https://doi.org/10.1007/978-3-319-58239-9_16, 2018.

Vörösmarty C.J., McIntyre P.B., Gessner M.O., Dudgeon D., Prusevich A., Green P., Glidden S., Bunn S.E., Sullivan C.A., Liermann C.R., and Davies P.M.: Global threats to human water security and river biodiversity, Nature, 467,555561, 10.1038/nature09440, 2010.

Walsh, C. J., Roy, A. H., Feminella, J. W., Cottingham, P. D., Groffman, P. M., and Morgan, R. P. : The urban stream syndrome: current knowledge and the search for a cure, Journal of the North American Benthological Society, 24(3), 706–723, https://doi.org/10.1899/04-028.1,2005.

Williams, G. P., and Wolman, M. G.: Downstream Effects of Dams on Alluvial Rivers, United States: U.S. Government Printing Office, https://doi.org/10.3133/pp1286,1984.
Wohl, E., and Merritt. D. M.: Reach-scale channel geometry of mountain streams, Geomorphology, 93, 168–185, https://doi.org/10.1016/j.geomorph.2007.02.014,2008.

Wohl, E., Bledsoe, B. P., Jacobson, R. B., Poff, N. L., Rathburn, S. L., Walters, D. M., and Wilcox, A. C.: The Natural Sediment Regime in Rivers: Broadening the Foundation for Ecosystem Management, BioScience,65,358–371, https://doi.org/10.1093/biosci/biv002,2015.

Wulder, M.A., White, J. C., Loveland, T. R., Woodcock, C. E., Belward, A. S., Cohen, W. B., Fosnight, E. A., Shaw, J., Masek, J. G., and Roy, D. P.: The global Landsat archive: Status, consolidation, and direction, Remote Sensing of Environment, 185, 271-283, https://doi.org/10.1016/j.rse.2015.11.032,2016.

Wulder, M.A., Loveland, T. R., Roy, D. P., Crawford, C. J., Masek, J. G., Woodcock, C. E., Allen, R. G., Anderson, M. C., Belward, A. S., Cohen, W. B., Dwyer, J., Erb, A., Gao, F., Griffiths, P., Helder, D., Hermosilla, T., Hipple, J. D., Hostert, P., Hughes, M. J., Huntington, J., Johnson, D. M., Kennedy, R., Kilic, A., Li, Z., Lymburner, L., McCorkel, J., Pahlevan, N., Scambos, T. A., Schaaf, C., Schott, J. R., Sheng, Y., Storey, J., Vermote, E.,Vogelmann,

https://doi.org/10.5194/egusphere-2026-6100
Preprint. Discussion started: 11 November 2026
© Author(s) 2026. CC BY 4.0 License.



J., White, J. C., Wynne, R. H.,and Zhu, Z.: Current status of Landsat program, science, and applications, Remote Sensing of Environment, 225,127-147, https://doi.org/10.1016/j.rse.2019.02.015, 2019.

Xu, H.: Modification of normalised difference water index (NDWI) to enhance open water features in remotely sensed imagery, International journal of remote sensing, *27*(14), 3025–3033, https://doi.org/10.1080/01431160600589179,2006.

Yadav, A., Boothroyd, R. J., Sambrook Smith, G. H., and Sen, S.: Morphological adjustments of the Yamuna River in the Himalayan foothills in response to natural and anthropogenic stresses, Hydrological Processes, *37*(7), https://doi.org/10.1002/hyp.14934,2023.